ChemPubSoc Europe
DOI: 10.1002/chem.201504396
CHEMISTRY
A European Journal
Review

Molecular Logic Gates

Anion Sensors as Logic Gates: A Close Encounter?

Madhuprasad,*[a] Mahesh P. Bhat,[a] Ho-Young Jung,[b] Dusan Losic,[c] and
Mahaveer D. Kurkuri*[a]

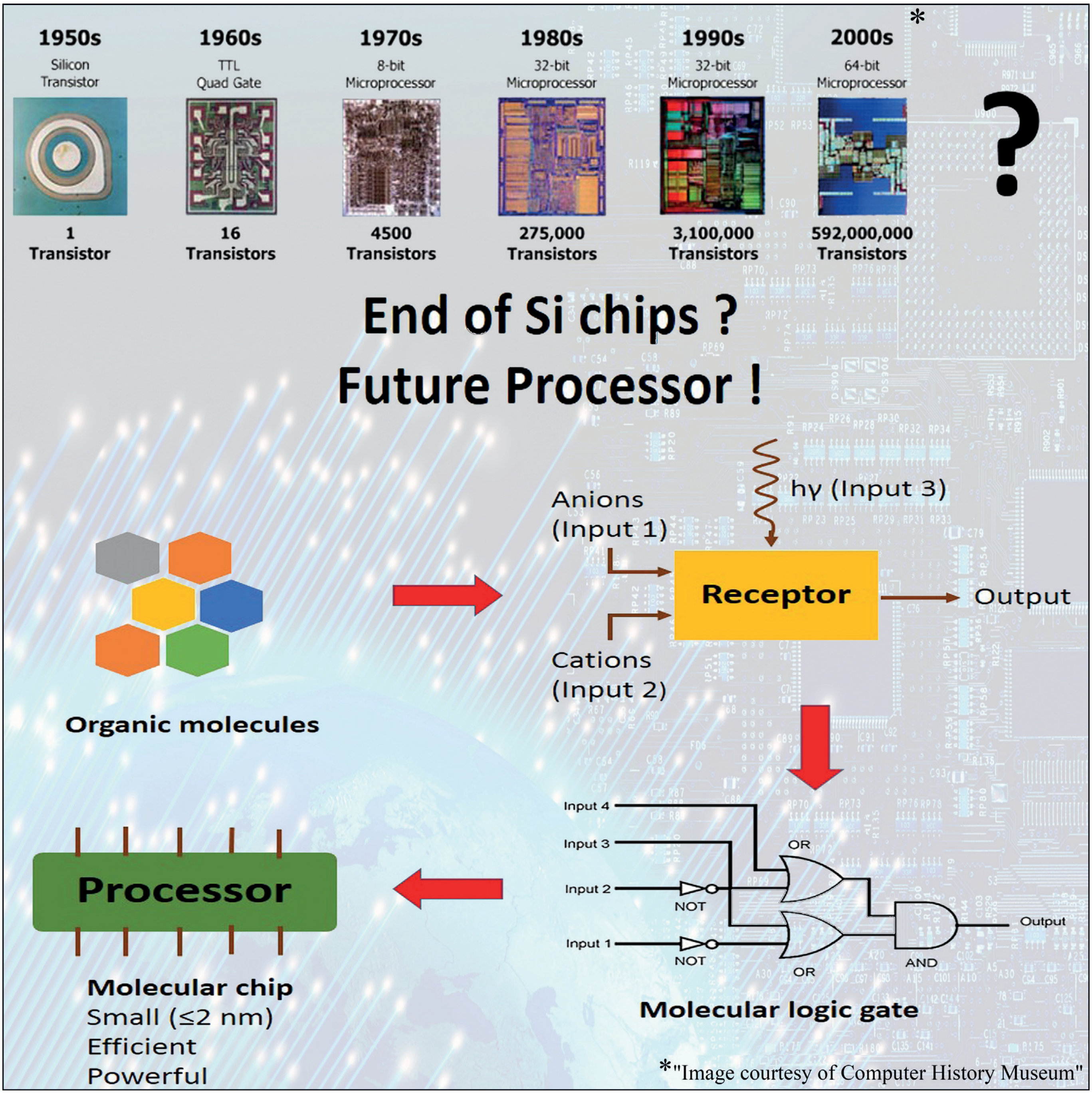

*"Image courtesy of Computer History Museum"

Abstract: Computers have become smarter, smaller, and more efficient due to the downscaling of silicon-based components. Top-down miniaturisation of silicon-based computer components is fast reaching its limitations because of physical constraints and economical non-feasibility. Therefore, the possibility of a bottom-up approach that uses molecules to build nano-sized devices has been initiated. As a result, molecular logic gates based on chemical inputs and measurable optical outputs have captured significant attention very recently. In addition, it would be interesting if such molecular logic gates could be developed by making use of ion sensors, which can give significantly sensitive output information. This review provides a brief introduction to anion receptors, molecular logic gates, a comprehensive review on describing recent advances and progress on development of ion receptors for molecular logic gates, and a brief idea about the application of molecular logic gates.

1. Introduction

Information technology (IT) has advanced significantly ever since the first digital/programmable computer was invented. Computers have become smarter, smaller and more efficient due to the downscaling of silicon-based computer components over a period of time. However, there is further scope to make the computer faster and more powerful—this could be achieved by making the active components in computer circuits smaller and denser through a miniaturised design process.[1] Conventional top-down miniaturisation of silicon-based computer components is reaching its limits due to physical constraints[2] and economical unfeasibility.[3] To address these limitations the researchers are looking into the possibilities of establishing bottom-up self-assembly molecular technology that uses atoms to build molecules of 1 or 2 nanometres in size.[4] As a result, molecular logic gates based on chemical inputs and measurable optical outputs have captured significant attention.

This review aims at reporting and compiling the most recent advances on anion-receptor-based molecular logic gates. Firstly we provide a brief introduction to molecular logic gates, the integration of organic molecules into molecular computation and anion receptors, followed by a comprehensive review on recent progress on establishing different concepts based on broad range of organic-ion-sensing molecules and their combination. Our specific focus is on molecular logic gates with combined ion sensors that showed high sensitivity and broad output information, and thus considered as great advancements in this field. Finally, we conclude this review with a general overview and a prospective outlook on the future trends, challenges and perspectives in this exciting and promising research field.

1.1. Molecular logic gates

Logic gates are the fundamental components of electronic and digital circuit. These logic gates perform logical operations in which they produce logical output signals with one or more logical input signals. These signals are represented in two binary conditions namely, low (0) and high (1) states, thus making them fundamental units of silicon-based computer components. Therefore, these logic gates are essential and unreplaceable components in the digital world. However, top-down miniaturisation of these components is limited owing to economical and physical restraints. Thus, to continue the Moore"s Law (doubling the number of transistors in an integrated circuit every two years) one has to explore new materials and/or new device architecture. Consequently, in a bottom-up approach, molecular logic gates could be used to make essential computer components, by converting chemical input signals into measurable output signals.

Bottom-up self-assembly molecular technology has been extensively explored to build and assemble molecules of 1 or 2 nanometres in size and then incorporate them into molecular logic gate devices.[4] Based on this bottom-up approach, the first example of molecular AND gate was established by de Silva et al. in 1993[5] and to this day the research group has published reports on a variety of molecular logic gates with various applications, including review articles.[6–11] Since then many materials, such as supramolecules, organic molecules, nucleic acids, proteins, DNA and polymers, have been used as input signals to mimic logic operations.[12–17] These molecular logic gates work as down-scaled switches that can be utilised in various states from solution to solid.[11,18–22] In recent years, increasing attention has been paid to the development of molecular logic gates based on anion/cation-detecting receptors. To establish these molecular logic gates, the output signals are measured in the form of change in absorbance/emission intensity with respect to various input signals, such as addition of ions or variation in the pH. The system is said to be switched “ON” if the absorbance/emission intensity is above a certain threshold level; if it is below the threshold level then system is said to be switched “OFF′. The ″switch-ON“ system is generally represented with Boolean operation ″1“ and the ″switch-OFF“ system is represented with Boolean operation ″0“. A number of logic gates have been established in which the addition of anions/cations provided the chemical input to get output sig-

[a] *Madhuprasad, M. P. Bhat, M. D. Kurkuri*
Centre for Nano and Material Sciences (CNMS)
Jain University, Jain Global Campus, Bangalore-562112 (India)
E-mail: madhuprasad@jainuniversity.ac.in
mahaveer.kurkuri@jainuniversity.ac.in

[b] *H.-Y. Jung*
Dept. of Environmental Energy Engineering
Chonnam National University, Gwangju 500-757 (Republic of Korea)

[c] *D. Losic*
School of Chemical Engineering, The University of Adelaide
North Engineering Building, Adelaide, SA-5005 (Australia)

nals. The majority of the discussion in this manuscript follow double input/single output logic gates in which two inputs (anion–anon, anion–cation and cation–anion) were used to get a single output. Therefore, it is good to take a look at all possible output patterns for double-input logic operations. A maximum of four input states for each inputs (Inputs 1 and 2) can be imagined and for each input state, an output state is obtained. Thus, the total number of input–output patterns that can be obtained is 16. These 16 patterns represents 16 different logic devices as shown in Table 1.

In this manuscript we aim to give a broad and comprehensive overview on logic gates established using anion as one of the inputs.

Table 1. Truth table for 16 different logic gates of double input/single output logic operations.

Input 1		0	1	0	1
Input 2		0	0	1	1
Output	PASS 0	0	0	0	0
	NOR	1	0	0	0
	INHIBIT 1	0	1	0	0
	INHIBIT 2	0	0	1	0
	AND	0	0	0	1
	NOT TRANSFER 1	1	1	0	0
	NOT TRANSFER 2	1	0	1	0
	XNOR	1	0	0	1
	XOR	0	1	1	0
	TRANSFER 1	0	1	0	1
	TRANSFER 2	0	0	1	1
	NAND	1	1	1	0
	reverse IMPLICATION	1	1	0	1
	IMPLICATION	1	0	1	1
	OR	0	1	1	1
	PASS 1	1	1	1	1

1.2. Integration of organic molecules into molecular computation

Firstly, it is important to understand that the molecular computation need not follow the same working principle as that of current semiconductor devices. Semiconductor devices can be connected with wires to control input/output signals. However, in molecular logics the input signal is controlled by several chemical parameters, such as addition of anions, cations, acids or other reagents, or by introducing physical parameters, such as UV/visible irradiation, temperature, or reaction conditions.[23,24] The output signals could be changes in emission/absorbance intensities, colour or conductance. Many chemicals and ions in biological systems could serve as inputs to molecu-

Dr. Madhuprasad received his Ph.D. degree in chemistry from National Institute of Technology Karnataka, Surathkal (India) in 2014. Later he joined Centre for Nano and Material Sciences as Senior Research Associate. His research area includes the design and investigation of colourimetric molecular sensors for anions/cations and synthesis of surface modified materials integrated with organic molecules for the removal of heavy metal impurities and hazardous anions.

Mahesh P. Bhat received his Bachelor of Science degree from S.D.M College, affiliated to Mangalore University (India) in 2012 and Master of Science degree in Analytical Chemistry from Department of Chemistry, St. Aloysius College, affiliated to Mangalore University (India) in 2014. Currently he is working as a research scholar at Centre for Nano and Material Sciences, Jain University (India). His main research focuses on design and fabrication of disposable devices for quantitative detection of fluoride in field studies.

Dr. Ho-Young Jung serves on the faculties of Environment & Energy Engineering at Chonnam National University (Korea). He obtained his Ph.D. in Chemical and Biomolecular Engineering at KAIST (Korea) in 2007. Prof. Jung's current work focuses on the development of advanced nanocomposite materials for the application to the energy conversion devices, such as fuel cells, redox flow batteries, ultrabatteries and water electrolyser systems. For redox flow batteries, new concepts of membrane materials with nano-filtered pores are actively studied with novel design and synthetic routes.

Prof. Dusan Losic is an Australian Future Fellow and Research Professor at the School of Chemical Engineering, The University of Adelaide (Australia), where he leads tha NanoResearch Group. He has completed his Ph.D. degree in Nanoscience and Nanotechnology at Flinders University (Australia) in 2003, where he worked as a Research Fellow, followed by a 5-year ARC Research Fellowship (2007) in the Ian Wark Research Institute at The University of South Australia. His multidisciplinary nanotechnology research involves fundamental, engineering and applied aspects across several disciplines, including chemistry, materials science, engineering, biology and medicine working on diverse topics, namely, molecular separations, biosensing and drug delivery.

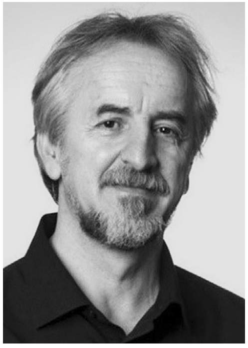

Dr. Mahaveer D. Kurkuri joined the Centre for Nano and Material Sciences, Jain University (India) as an Associate Professor in 2014 and holds a visiting staff position at School of Chemical Engineering, The University of Adelaide (Australia). He received his Ph.D. degree in Polymer Chemistry from Karnataka University, Dharwad (India) in 2003. He has published more than 25 papers in peer reviewed journals. His current research interests are microfluidics, biosensors, surface chemistry, in general to mimic the nature, particularly utilising the understandings in nano and bio areas.

lar logic gates. In addition, electrochemical variations can also be served as inputs in molecular logic components along with the combination of semiconductor devices.

Optical input systems such as irradiation of UV and visible light have been used as different inputs to develop logic gates. For instance, molecular transport junctions (MTJs) have been investigated by chemical tailoring of a ruthenium complexed binuclear photochromic organic molecule to gold nanowires to fabricate a nanoelectrodes.[25] These molecular wires with photosensitive organometallic complexes undergo photoisomerisation between the π-conjugated closed state and the non-conjugated open state, which leads to conductive nanodevice (Figure 1).

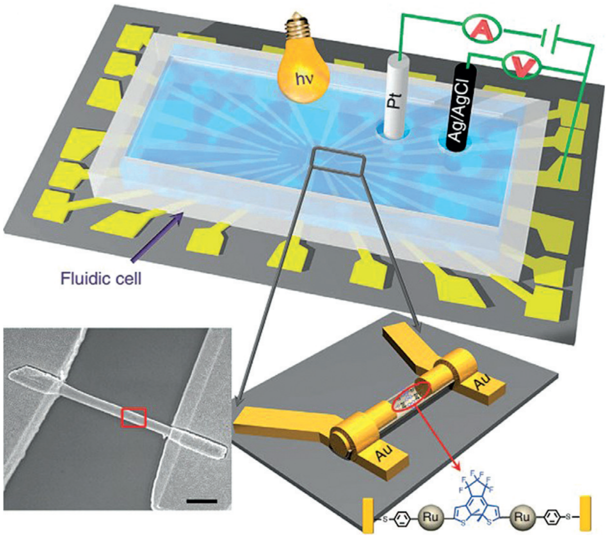

Figure 1. Illustration of functionalised nanogap devices. Inset: SEM image of a real device fabricated from an on-wire lithography generated nanowire (scale bar: 1 μm) (reproduced from reference [25], with permission from Nature).

This MTJ can be used as molecular logic device in which UV light irradiation and electrochemical stimulus are employed as two inputs. The presence and absence of each input is designated as Boolean operation "1" and "0", respectively. Presence of either inputs or both inputs triggers the formation of the π-conjugated closed state from non-conjugated open state, resulting in the enhancement of the device conductivity. Thus, the device mimicked a Boolean operation corresponding to an OR gate (Figure 2b and c). The device could be reset to its original state just by irradiating visible light at 700 nm as shown in Figure 2a. This work has been further extended to develop multi-addressable MTJs for advanced and complicated molecular computing.

We know that physical integration of molecular logic devices is practically difficult. For example; the change in fluorescence intensity that is an output from one molecular logic gate is difficult to use as an input into a second logic gate. This type of joining-up is easy in case of larger semiconductor devices as they can connect with wires to different devices. On the other hand, in molecular logic devices this joining-up could be avoided by conducting chemical experiments in one pot. For example; colourless $[Fe(CN)_5NO]^{2-}$ reacts with organic thiols (RSH) to give purple $[Fe(CN)_5N(O)SR]^{3-}$. This purple complex absorbs light at 520 nm, which is considered to be an output. The complex is stable only if the concentration of K^+ is high and concentration of H^+ is low. Therefore the overall output can be controlled by varying these two ions and thus the final obtained output represents an INH logic gate. When we combine two cells containing this complex, either of these cells or both of them may produce the purple complex. Therefore, when two cells containing the complex are placed together, the overall output changes from INH to OR logic (Figure 3).[23]

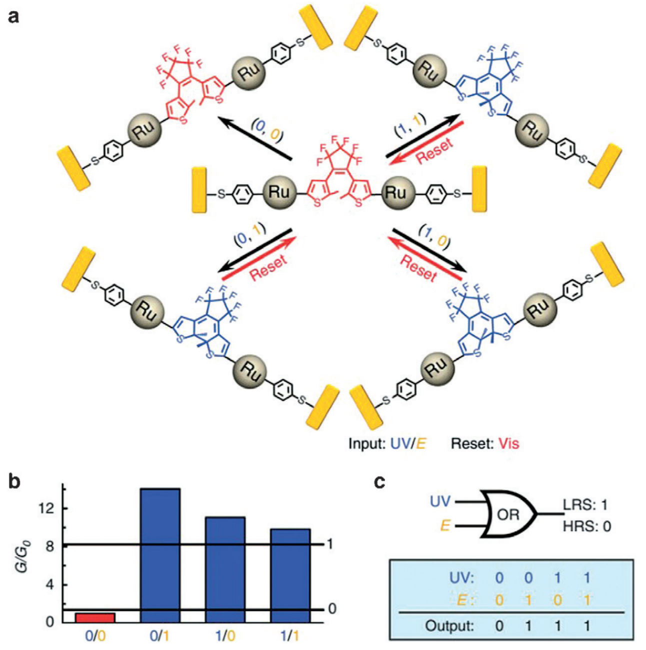

Figure 2. Resettable OR logic gate using an MTJ. a) Scheme of logic gate: isomerisation within nanogap devices under UV irradiation and electrolysis inputs. Reset: visible light irradiation (700 nm). b) Conductance changes with different input combinations. c) Truth table of OR logic gate (reproduced from reference [25], with permission from Nature).

In addition to the above illustrations, several other nanocell logic gates for molecular computing have been discussed in the literature.[26]

1.3. Anion sensors

Anions are deeply associated with vibrant applications in various industrial, biological, chemical and environmental processes[27,28] along with many other important aspects of chemistry.[29–33] Consequently, organic receptors with neutral binding, sites such as urea/thiourea, amide pyrrole, aminopyrrole, indole and hydroxyl groups,[27,28,34–46] with cationic units, such as ammonium, quinolinium, imidazolium and guanidinium salts,[47–51] and sensors with active methylene groups[52–54] have been used for anion detection. In addition, anion-induced reactions, such as desilylation[55,56] and nucleophilic interactions,[57–61] have also been used for the anion detection. Many anion sensors have been utilised for significant applications,

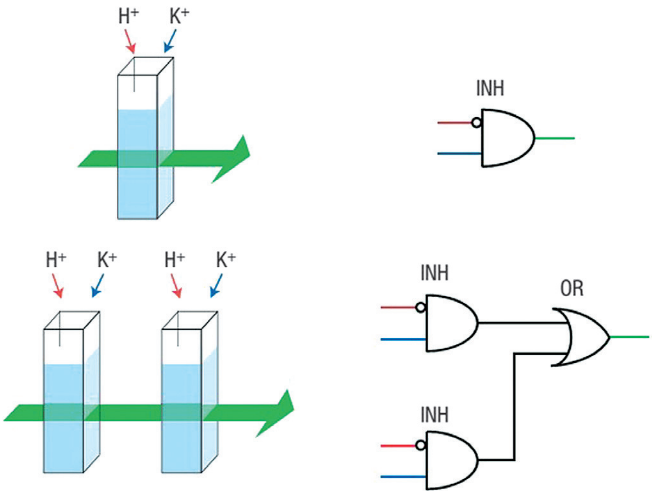

Figure 3. Integrated molecular logic gates based on colour-forming reactions. Top: Sodium salt of $[Fe(CN)_5NO]^{2-}$ reacts rapidly with RSH to generate the purple $[Fe(CN)_5N(O)SR]^{3-}$ only if H^+ concentration (red input channel) is low and K^+ concentration (blue input channel) is high. The output measured at 520 nm represents an INH logic gate. Bottom: Measuring the absorbance through two cells in series produces a result interpretable as a more complex logic gate array of two INH gates feeding their outputs into an OR gate (reproduced from reference [23] with permission from Nature).

such as detection of cancer cells,[62] determination of percentage composition in binary solvent mixtures,[63] detection of water contaminants,[53,54] anion-detecting strips[64,65] and smart molecules.[66–68] In addition, these anion sensors have been used to develop computing components, such as molecular logic gates, which will be explained in-detail in the following text. The advantage of anion sensors as a molecular components is their selectivity[62,69–71] when compared to cation sensors (generally only one anion can be recognised with one receptor). In addition, these anion sensors are easily reversible to its original state by treating the anion complex with acids.[72]

2. Anion Input Logic Gates

In this section only anion receptors are discussed that were explored as chemical inputs to get output signals in the form of change in colour, absorbance or emission. The binding priority of the anions is responsible for this change. In this section we will discuss specifically about the establishment of logic gates in which the addition of anions provide two or more chemical inputs.

Imidazolium systems bearing two pyrene groups have been synthesised and the binding properties of these systems have been examined with respect to fluorescent changes.[73] The fluorescent changes of host **1** upon the addition of different anions have been studied; the host showed significant quenching of fluorescence for $H_2PO_4^-$ ions. On addition of an excess of $H_2PO_4^-$ ions to compound **1**, a blue-shifted excimer emission was observed upon excitation, owing to formation of a pyrene dimer in the ground state (static excimer).

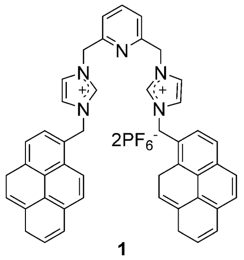

1

This imidazolium-based compound has been used for molecular logic gate applications. Compound **1** displays a large fluorescent quenching upon the addition of OH^- (100 equiv) in acetonitrile and the addition of an even higher concentration of OH^- (1000 equiv) induced a fluorescent quenching effect of the excimer peak. However, the fluorescent intensity due to the monomer emission increased significantly. Therefore, the addition of OH^- ions at different concentrations was considered as two different chemical inputs. The output signals were recorded at two different wavelengths, thus giving two different logic functions. Accordingly, based on the amounts of OH^- added, two output signals corresponding to AND (Output 1) and NOR (Output 2) functions (Table 2 and Figure 4) were obtained. In addition, compound **1** showed enhancement in the fluorescence upon adding trifluoroacetic acid (TFA). This was ascribed to the partial blocking of photo-induced electron transfer (PET) mechanism due to the protonation of nitrogen in the pyridine ring. However, no change in the quenching effect was observed upon adding both OH^- as well as TFA. This quenching and enhancement were utilised to develop a third logic gate whereby the addition of OH^- and TFA provided two chemical inputs to give an output signal corresponding to INH logic gate (Table 2 and Figure 4).

Table 2. Truth table corresponding to AND, NOR and INH logic gates.

Input 1 (OH^-)	Input 2 (OH^-)	Output 1 (395 nm) AND	Output 2 (478 nm) NOR	Input 1 (OH^-)	Input 2 ($H+$)	Output 2 (478 nm) INH
0	0	0	1	0	0	0
1	0	0	0	1	0	0
0	1	0	0	0	1	1
1	1	1	0	1	1	0

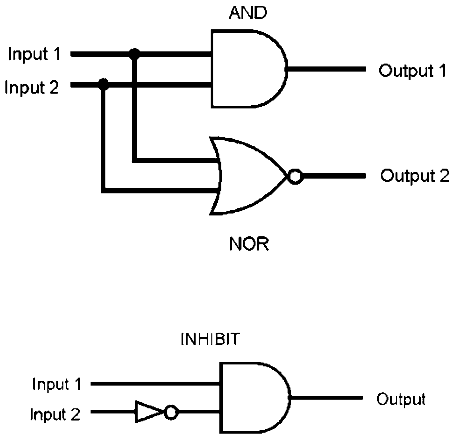

Figure 4. AND, NOR and INH logic gates established with two chemical input system.

A chemosensor **2**, based on thiosemicarbazide, has been synthesised for the detection of F^- ions.[74] It has been found that a solution of this sensor in DMSO is highly selective toward F^- ions in both UV/Vis and fluorescence spectroscopy. Upon adding F^- ions to the chemosensor in DMSO, a significant colour change from colourless to yellow was observed. Surprisingly, the F^--induced chromogenic process is totally reversible with the addition of HSO_4^- ions, which was evidenced by UV/Vis spectroscopy—the vanishing of an absorption band at 421 nm and reappearance of the absorption at 348 nm was observed upon addition of HSO_4^- ions (Figure 5).

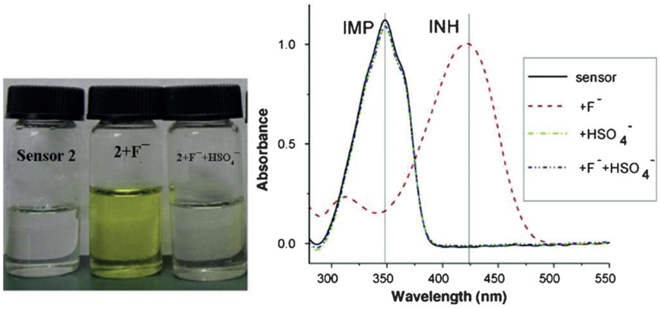

Figure 5. Left: Colour change of **2** upon addition F^- and HSO_4^- in DMSO. Right: Corresponding UV/Vis change in DMSO (reproduced from reference [74] with permission from Elsevier).

The reversible colourless–yellow–colourless cycle can be repeated several times by adding 5 equivalents of F^- and 1.5 equivalents of HSO_4^- ions. This result indicates that the presence of HSO_4^- anions would inhibit the interaction of F^- with the chemosensor **2**, as HSO_4^- is more acidic compared to chemosensor **2**. As illustrated in Figure 6, the interaction of HSO_4^- with the chemosensor:F^- complex reproduces the chemosensor.

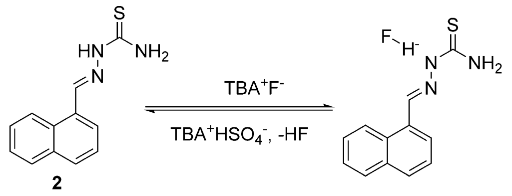

Figure 6. Mechanism of F^- ion binding to form a chemosensor:F^- complex and the reverse reaction upon treatment with HSO_4^- ion.

This reversible colourimetric switching process can be represented by a molecular logic gate, employing F^- (Input 1) and HSO_4^- (Input 2) as the input signals and the absorbance at 348 nm and 421 nm as the output signals (Table 3). These output signals represent IMP and INH logic gates (Figure 7 a). Hence, the colour changes of chemosensor **2** in DMSO (optical output) are controlled by the input of two anions namely, "switch-ON′" by adding F^- ions and "switch-OFF" on adding HSO_4^- ions.

Table 3. Truth table corresponding to IMP and INH logic gates and to the logic circuit of a memory machine.

Input 1 (F^-)	Input 2 (HSO_4^-)	Output 1 (348 nm) IMP	Output 2 (421 nm) INH	Set (F^-)	Reset (HSO_4^-)	Output 2 (421 nm)
0	0	1	0	0	0	0
1	0	0	1	1	0	1
0	1	1	0	0	1	0
1	1	1	0	1	1	0

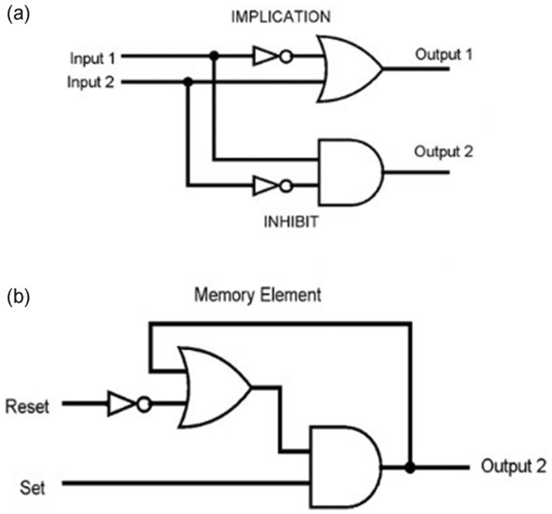

Figure 7. a) Logic circuit for IMP and INH gates. b) Logic circuit for a memory machine.

Based on reproducible colourimetric switching, a useful sequential logic circuit has been designed that shows memory machine properties by following "writing–reading–erasing–reading" behaviour in molecular-level information processing. This behaviour was studied by using "set" (addition of F^-) and "reset" (addition of HSO_4^-) inputs. The operation of this memory machine is shown in Table 3. Further, based on the output signals, a logic circuit corresponding to the memory machine was achieved (Figure 7 b) that displayed a molecular switch with an "ON–OFF" property. More significantly, this "ON–OFF" behaviour was repeatable many times over, which suggested "writing–reading–erasing–reading" cycles.

A new red-emission diketopyrrolopyrrole (DPP)-based chemosensor **3** with two strong electron-donating triphenylamine groups has been designed and synthesised for the colourimetric detection of F^- ions.[75] The sensing properties of chemosensor **3** for F^- ion have been investigated in acetone and in acetonitrile. A significant colour change from red to purple in ambient light was observed in both the solvents upon addition of F^- ions. The change in colour was attributed to the deprotonation of the N–H group in chemosensor **3**. In addition to colourimetric detection, chemosensor **3** showed distinct fluorescent changes with dual mode approaches namely, "ratiometric" and "turn-on" modes in acetone and acetonitrile, respectively. In acetone, the "ratiometric" channel was activated upon addition of F^- ions, resulting in a bathochromic shift from 590 nm to 641 nm along with an emission colour change from orange to purple-red. In acetonitrile, a "turn-on" response with red emission at 631 nm was observed along with a 50-fold fluorescence enhancement.

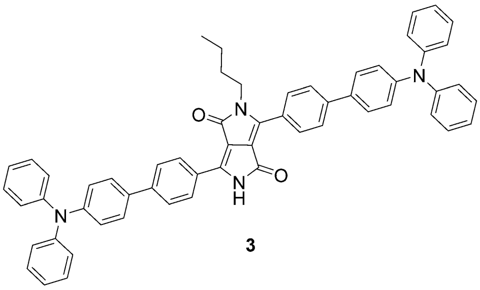

3

The absorption spectra of chemosensor **3** in the presence of F^- (Input 1) and HSO_4^- (Input 2) was recorded and the spectrum of chemosensor **3** showed a broad peak, with an absorption maxima at around 520 nm. After adding F^- (Input 1 = 1, Input 2 = 0), chemosensor **3** displayed a new absorption band at 594 nm (Output = 1). However, as shown in Figure 8a, no change was observed on the addition of HSO_4^- even in presence of F^- (Input 1 = 0, Input 2 = 1 and Input 1 = 1, Input 2 = 1). The truth table evidently suggests that the operation of chemosensor **3** with F^- and HSO_4^- inputs expresses the INH logic gate function. Further, chemosensor **3** was demonstrated to act as an INH logic gate with emission at 631 nm as the output signal and F^-/HSO_4^- as input signals. Chemosensor **3** is not fluorescent in acetonitrile (Input 1 = 0, Input 2 = 0; Output = 0), and the system did not show any fluorescence change upon addition of HSO_4^- with and without F^- (Input 1 = 0, Input 2 = 1 Output = 0 and Input 1 = 1, Input 2 = 1; Output = 0). However, on addition of only F^- ions (30 equiv), a 50-fold enhancement (Figure 8b) in the fluorescence emission at 631 nm was observed (Input 1 = 1, Input 2 = 0; Output = 1).

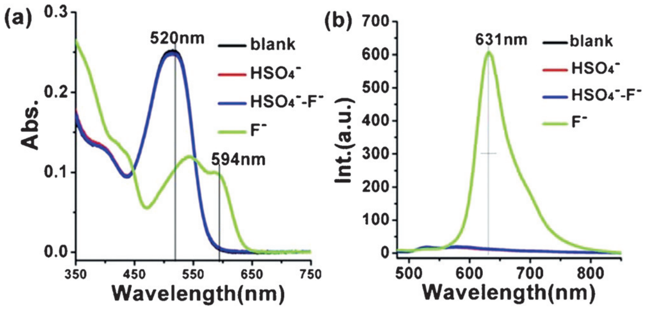

Figure 8. a) Absorption and b) emission spectra of **3** on adding 30 equiv of F^- and HSO_4^- in MeCN (reproduced from reference [75] with permission from Elsevier).

Thus, using F^- and HSO_4^- ions as two chemical inputs and absorption or fluorescence as output, two-input/two-output INH logic gate has been achieved (Figure 9).

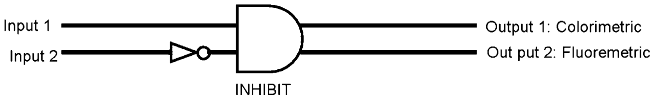

Figure 9. Logic circuit for INH gates.

A naphthalenediimide (NDI)-based receptor **4** has been designed and synthesised by Mukhopadhyay and co-workers for the detection of F^- ions.[76] Receptor **4** in dry DMF, experienced deprotonation reactions at the hydrazimide NH positions upon the addition of an excess of tetrabutylammonium fluoride (TBAF) to give an intense green solution.

This significant change in the colour is perhaps due to the establishment of intramolecular charge transfer (ICT). On the other hand, upon addition of only 5 equivalents of TBAF to a solution of receptor **4** in DMF the solution turned brown. This is owing to the formation of a NDI radical anion, which resulted in a single electron transfer (SET) transitions. Finally if a large excess of TBAF with trace amounts of water was added to a solution of the receptor in DMF, the solution gradually turned blue. This observation was attributed to the formation of the dianion of NDI, which results in the establishment of double electron transfer (DET). The Figure 10 shows colour change of receptor **4** during the detection process.

Figure 10. Colour change upon adding TBAF in different concentrations to receptor **4**; a) receptor solution, b) formation of the ICT state in excess of TBAF, c) formation of SET state on adding 5 equiv of TBAF in DMF and d) formation of DET state on adding 30 equiv of TBAF in DMF/H_2O (99:1 v/v) (reproduced from reference [76] with permission from the RSC).

Thus, establishment of four stable molecular states was achieved (Figure 11), which enabled the generation of simple logic gates, such as AND, XOR and INH, along with combinational logic gates like a three-input AND gate, a half-adder and a 1:2 demultiplexer.

To demonstrate the three-input AND logic gate, addition of 5 and 10 equivalents of TBAF provided the first two inputs (Inputs 1 and 2) and the addition of H_2O was used as the third input (Input 3). The output signal was recorded as the change in intensity of absorbance at 348 nm. The "ON" state of the logic gate was made possible only with the DET reaction, as

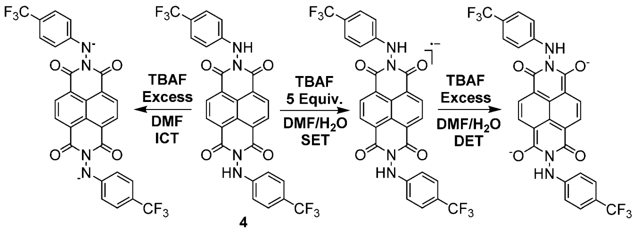

Figure 11. Four states of receptor **4**; neutral, deprotonated, radical anion and dianion.

Table 4. Truth table corresponding to an AND logic gate with a three-input system.

Input 1 (F^- 5 equiv)	Input 2 (F^- 10 equiv)	Input 3 (H_2O)	Output (348 nm) AND
0	0	0	0
1	0	0	0
0	1	0	0
0	0	1	0
1	1	0	0
1	0	1	0
0	1	1	0
1	1	1	1

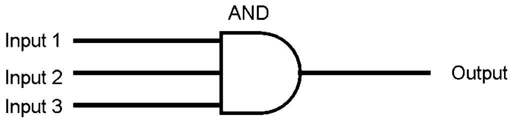

Figure 12. Logic circuit for an AND gate with a three-input system.

the dianion could be formed with the addition of all three inputs (Table 4). On compiling the output signals from the three-input signals a logic circuit for the AND gate was obtained (Figure 12).

By using 10 equivalents of TBAF in DMF as the chemically degenerate inputs Inputs 1 and 2, a half-adder logic gate was demonstrated. The truth table (Table 4) for the half-adder logic circuit was established by monitoring the multichannel signal read-outs at 347 nm or 645 nm (ICT) and 472 nm or 774 nm (SET).

Receptor **4** delivered an output signal corresponding to a XOR gate upon the addition of 10 equivalents of TBAF, which triggered the SET reaction (radical anion state). However, the addition of TBAF also triggered the deprotonation reaction to establish ICT and thus to give an output signal corresponding to AND gate. Combining the output signals a half-adder logic circuit was achieved as shown in Figure 13 a.

Finally, a 1:2 demultiplexer logic circuit (Figure 13 b) was established that processes one data input (Input 1), one address input (Input 2) and one output. Receptor **4** in DMF was treated with 30 equivalents of TBAF, which is considered as the data input (Input 1), and the addition of H_2O is considered as the address input (Input 2). Receptor **4** with the TBAF input in DMF established the ICT transition, which provided the output signal corresponding to an INH gate. However, the addition of water together with TBAF resulted in the DET reaction and this delivered the output signal corresponding to an AND gate (Table 5).

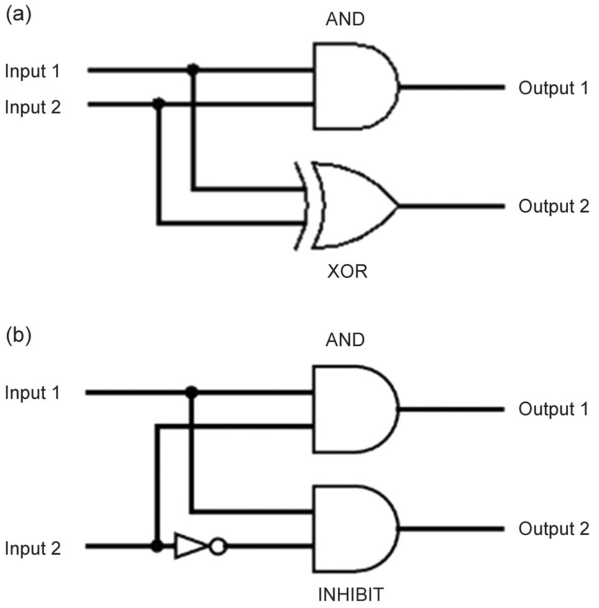

Figure 13. a) Half-adder logic circuit for AND and XOR gates. b) Demultiplexer logic circuit for AND and INH gates.

Table 5. Truth table corresponding to AND and XOR gates with different concentrations of F^- ions as inputs and the truth table corresponding to INH and AND gates with F^- ions and H_2O as inputs.

Input 1 (F^- 10 equiv)	Input 2 (F^- 10 equiv)	Output 1 AND	Output 2 XOR	Input 1 (F^- 30 equiv)	Input 2 (H_2O)	Output 1 INH	Output 2 AND
0	0	0	0	0	0	0	0
1	0	0	1	1	0	1	0
0	1	0	1	0	1	0	0
1	1	1	0	1	1	0	1

An organoeuropium complex **5** containing dibenzoylmethane and dipyrido[3,2-*a*:2′,3′-*c*]phenazine has been synthesised and the photophysical properties of this complex have been described.[77] The europium complex **5** was able to effectively recognise the AcO^- ion over other anions with an increase in luminescence intensity.

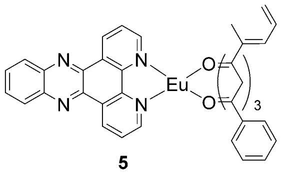

5

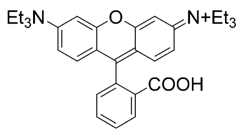

6

The detection mechanism was attributed to the replacement of dipyrido[3,2-*a*:2′,3′-*c*]phenazine by an AcO^- ion. In addition, on introducing molecular oxygen to complex **5**, a significant change in the Eu^{3+} emission was observed. This observation was ascribed to a thermally activated back-energy transfer between the $^5D_0$ level of the Eu^{3+} ion and the triplet energy level of dipyrido[3,2-*a*:2′,3′-*c*]phenazine ligand. These characteristic properties of complex **5** successfully enabled the mimicking of an IMP gate with addition of AcO^- ion as Input 1 and the introduction of molecular oxygen as Input 2—the intensity of photoluminescence was considered as the output signal. The photoluminescence quenching was observed only in the absence of AcO^- under oxygen atmosphere to give an output signal "0" and under other circumstances the luminescence of the europium complex **5** was enhanced, thus giving an output signal of "1".

An efficient colourimetric and fluorometric chemosensor **6**, based on Rhodamine B (RhB), for the detection of cyanide ions in an absolutely aqueous media has been developed.[78] Chemosensor **6** is a fluorescent molecule that shows a strong emission band at 578 nm in H_2O. Upon the addition of phosphotungstic acid ($H_3PW_{12}O_{40}$ or PTA) a significant quenching of the emission spectra was observed and simultaneously the colour of the solution changed from pink to purple. This quenching and colour change is caused by the formation of an $(RhB^+)_3{\cdot}PTA^{3-}$ complex, which can be used to detect CN^- ions in aqueous media. Upon addition of CN^- ions to the $(RhB^+)_3{\cdot}PTA^{3-}$ complex, a restoration of the strong fluorescence emission along with the colour change from purple to pink is observed: thus the system can exhibit "ON–OFF–ON" behaviour. The process of colour change and the mechanism is summarised in Figure 14.

Furthermore, the "ON–OFF–ON" function of the system was repeated several times to verify the reproducibility. Thus, the reversible and reproducible system was implemented to logic gate applications. The PTA and CN^- ions were used as two inputs (Inputs 1 and 2, respectively) and the change in emission intensity recorded at 578 nm was taken as the output signal. On combining two inputs, an output signal corresponding to IMP logic gate was obtained.

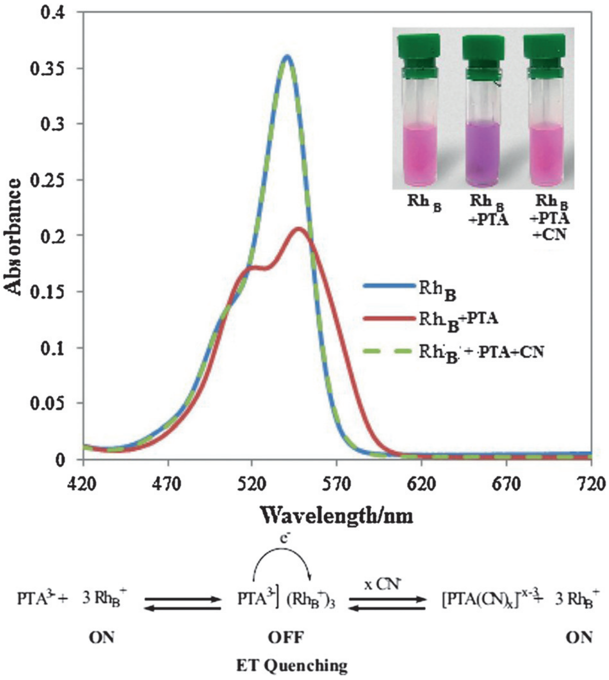

Figure 14. Top: UV/Vis spectra of RhB in aqueous solution with combinations of PTA and CN^- ions; Inset: Colour change; RhB, RhB with PTA and $(RhB^+)_3{\cdot}PTA^{3-}$ with CN^- ion (left to right). Bottom: Binding mode of RhB in the presence of PTA and CN^- in aqueous media (reproduced from reference [78] with permission from Elsevier).

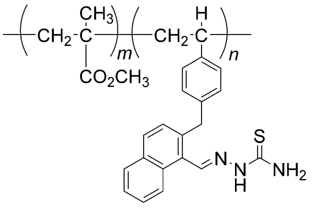

7

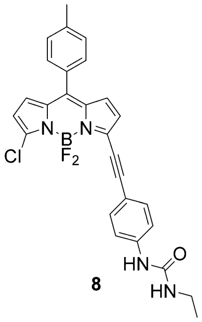

8

A unique polymer poly(MMA-co-VNT) **7** with different functional units, a predetermined molecular weight, and a narrow molecular-weight distribution was synthesised by copolymerising a styryl-type monomer, 2-(4-vinylbenzyloxy)-1-naphthaldehyde thiosemicarbazone (VNT) with methyl methacrylate (MMA).[79] This polymer was examined for the detection of anions, for which it showed a high selectivity to F^- ions over other anions. On addition of F^- ion to a solution of polymer **7** in DMSO, a significant colour change from colourless to yellow was observed. The signalling mechanism for the polymeric sensor is related to the deprotonation process of thiosemicarbazone lateral groups.

However, upon adding HSO_4^- ions to the polymer:F^- complex the colour of the solution reverted back to its original colour (Figure 15). Thus, the colourimetric detection process of polymeric sensor **7** could be swapped back and forth by successively adding F^- ions and HSO_4^- ions to the solution of the polymer in DMSO. Based on this reversible and reproducible sensing system, a molecular-scale sequential information processing circuit was designed that displays "writing–reading–erasing–reading" properties and "multi-write" functions in the form of binary logic. To demonstrate the logic gate circuit, addition of F^- ions and HSO_4^- ions provided Inputs 1 and 2, respectively, whereas the absorption measured at 365 nm and 425 nm provided Outputs 1 and 2, respectively. The signals at Output 1 are correspond to the IMP logic gate circuit and the signals at Output 2 resemble the INH logic gate circuit.

A colourimetric and fluorescent sensor **8** based on BODIPY with a urea group attached has been synthesised.[80] Sensor **8** showed significant selectivity and sensitivity toward F^- ions among many other anions. Upon addition of F^- ions, the absorption maxima of sensor shifted from 581 nm to 588 nm. This bathochromic shift resulted in a colour change from pink

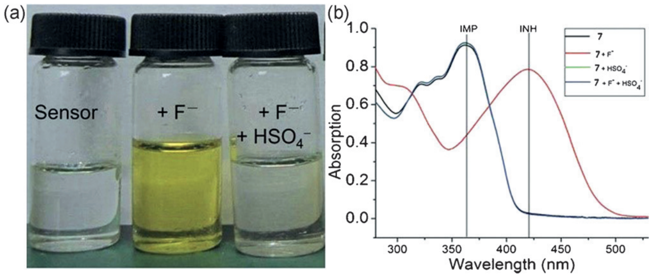

Figure 15. a) Colour change and b) change in UV/Vis spectra of **7** with various combinations of F^- and HSO_4^-, representing molecular IMP (365 nm) and INH (425 nm) logic functions (reproduced from reference [79] with permission from Wiley-VCH).

to blue; however, other ions did not induce any colour change. Further, upon excitation of **8** at 550 nm, the intensity of fluorescent emission at 608 nm was quenched by 87 %.

The absorbance and fluorescence emission of the **8**:F^- complex is reversible only on subsequent inclusion of HSO_4^- ions. This reversibility also resulted in the restoration of original colour (Figure 16). These results were taken together to develop a well-defined anion-induced logic gate.

The addition of F^- ions and HSO_4^- ions provided the two inputs (Inputs 1 and 2). The changes in intensities of fluorescence at 608 nm and absorbance at 610 nm were considered as Outputs 1 and 2, respectively. Upon adding F^- ions the fluorescence emission quenched and on adding HSO_4^- ions to the same solution the quenched fluorescence emission was restored. Thus, this represents an IMP logic circuit. Furthermore, an INH logic circuit was established by using the output information at Output 2.

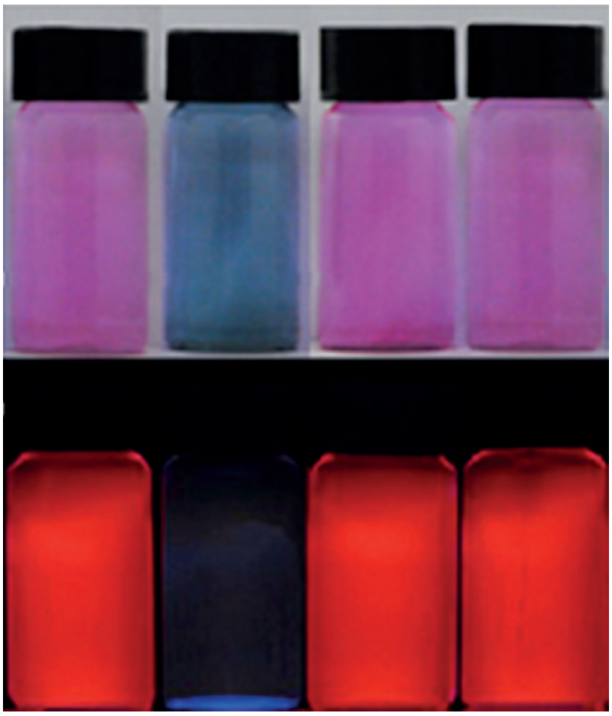

Figure 16. colourimetric and fluorometric change of **8** upon adding anions. Left to right: **8**, **8** + F^- ions, **8** + HSO_4^- ions and **8** + F^- + HSO_4^- ions (reproduced from reference [80] with permission from Elsevier).

In addition to the simpler molecular logic gates, very complicated logic circuits can be developed[74,76] for various applications. However, if one has to apply these logical units for biological and intracellular applications it is important to make these molecules water soluble. On the other hand, these organic molecules could be applicable in ecological monitoring devices. Organic compounds that have ionic salts, such as imidazolium ions,[73] could be used to monitor intracellular ion concentrations.

3. Anion–Cation Input Logic Gates

This section reviews logic gate systems that have been established by using the addition of anions as chemical Input 1 and addition of cations as chemical Input 2. Change in absorbance, fluorescence or sol–gel state is considered as output signal.

A compound **9**, comprising 2.2′-binaphthol coupled with benzimidazole moieties, has been examined for the establishment of a half-subtractor logic operation.[81] On excitation at 330 nm, compound **9** displayed strong fluorescence at 585 nm attributing to excited state intramolecular proton transfer (ESIPT) from phenolic OH to benzimidazole nitrogen, and was quenched completely upon addition of perchloric acid ($HClO_4$). Simultaneously, a new emission band at 435 nm appears. On the other hand, upon addition of tetrabutylammonium hydroxide (TBAOH) to a solution of compound **9** in acetonitrile, a new emission band at 515 nm with gradual quenching at 585 nm was observed. The quenching process is reversed on addition of $HClO_4$. Thus, compound **9** showed a large discrepancy in the emission spectra under various conditions (neutral, acidic and basic), which provided multiple prospects for the half-subtractor logic operations. A half-subtractor is nothing but a combinatorial circuit that subtracts two bits to produce their difference. It requires two output signals: one produces the difference (D) and the other generates borrow (B). These outputs could be thus produced by XOR and INH gates, respectively. The addition of $HClO_4$ (H^+) and TBAOH (OH^-) provided the two inputs (Inputs 1 and 2, respectively). The variation in the intensities of emission spectra at 435 nm, 515 nm and 475 nm provided the output signals (Output 1, 2 and 3, respectively). The results are compiled in the Table 6 and with two inputs, and outputs corresponding to INH (at 435/515 nm) and XOR (475 nm) gates were obtained. A schematic representation of a half-subtractor logic circuit is given in Figure 17.

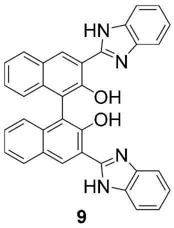

9

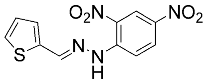

10

Table 6. Truth table corresponding to INH and XOR logic gates with different inputs.

Input 1 (H^+)	Input 2 (OH^-)	Output (435 nm) INH	Output (515 nm) INH	Output (475 nm) XOR
0	0	0	0	0
1	0	1	0	1
0	1	0	1	1
1	1	0	0	0

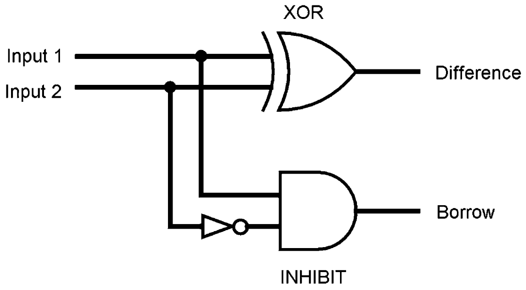

Figure 17. Logic circuit for XOR and INH gates.

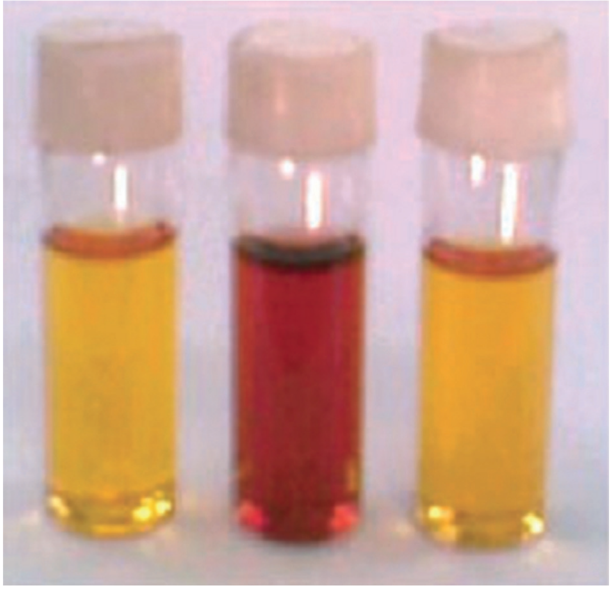

Figure 18. Colour changes of receptor **10**. Left to right: in the absence of ions, in the presence AcO^- ions and in presence of AcO^- along with Zn^{2+} (reproduced from reference [82] with permission the RSC).

The output signals at 435/515 nm correspond to an INH gate and that at 585 nm represents a XNOR gate. These have been elaborated as combinatorial logic circuits for a molecular half-subtractor with $HClO_4$ and TBAOH as input variables.

A thiophene–hydrazone-based receptor **10**, which acts as a colourimetric receptor for F^- ions and AcO^- ions has been synthesised.[82] Upon addition of AcO^- ions to a solution of **10** in DMSO, the peak due to the π–π^* transition at 407 nm disappears gradually and a new band at 505 nm appears. Simultaneously, the colour of receptor **10** changes from orange to dark red. Furthermore, on addition of 10 equivalents of Zn^{2+} to the same solution (receptor **10**:AcO^-) the red colour of solution disappears to restore the original orange colour of receptor **10** (Figure 18).

This colour change was evidenced by UV/Vis spectroscopy, in which the absorption band at 505 nm disappeared and the absorption band at 407 nm reappeared. The colour changes (optical outputs) were controlled by inputs of anion and cation; the AcO^- switches the optical output to "ON", while Zn^{2+} switches it to "OFF". An expedient way of representing these optical changes is through a molecular logic gate. The changes in absorbance at 407 nm and 505 nm were considered as outputs (Outputs 1 and 2, respectively) in response to the inputs. The output signals recorded at 407 nm (Output 1) are in accordance with an IMP logic gate and the spectral changes considered at 505 nm (Output 2) correspond to an INH logic gate.

Photophysical properties of new azobenzene comprising compounds (*E*)-2-[{2-(undec-10-enoyloxy)phenyl}diazenyl]phenol (**11**) and 2-[(*E*)-{2-((*E*)-3-bromoallyloxy)phenyl}diazenyl]phenol (**12**) have been examined at various pH levels.[83] Large differences in their sensing characteristics toward metal ions were observed. An exclusive selectivity and sensitivity to Zn^{2+} ion with a significant change in colour (light yellow to reddish orange) was observed for compound **11**. On the other hand, when compound **12** was treated with different metal ions it showed a change in colour and corresponding absorption spectra for Co^{2+}, Cu^{2+}, Pd^{2+} and Ni^{2+}. Thus, to investigate the selectivity of compound **12** toward metal ions, fluorescence spectra were recorded for which only Cu^{2+} and Pd^{2+} ions showed enhancement in the fluorescence intensity at 400 nm. The reversibility of compound **12** was investigated in two pH values: pH 7.0 and pH 10.5 by treating it with strong chelating agent EDTA. Variation in the pH has been considered as Input 1, the addition of Zn^{2+} as Input 2 and fluorescence intensity at 610 nm was taken as the output. An output signal corresponding to INH has been obtained on introduction of two inputs.

Similarly, the reversibility of compound **12** was examined in two pH values: pH 7.0 and pH 12. The addition of OH^- and

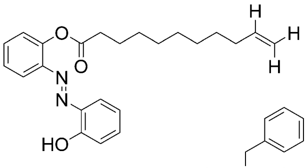

11

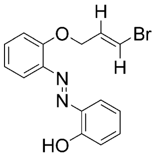

12

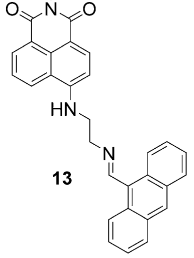

13

Cu^{2+} provided the input signals and the fluorescence intensity at 410 nm was considered an output signal. At pH 7.0 (i.e., Input 1 = 0 and Input 2 = 0) the output signal = 0 was recorded and in all other cases it was = 1. Thus, an output signal corresponding to an OR gate was obtained (Table 7), which is represented in Figure 19.

Table 7. Truth table corresponding to an OR logic gate.

Input 1 (OH^-)	Input 2 (Cu^{2+})	Output (610 nm) OR
0	0	0
1	0	1
0	1	1
1	1	1

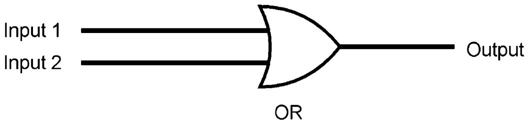

Figure 19. Logic circuit corresponding to an OR gate.

A fluorescent bischromophoric compound **13** for F^- and Hg^{2+} ions has been synthesised by combining anthracene and naphthalic imide.[84] The anion-binding ability of compound **13** was examined by treating it with different anions such as, in F^-, Br^-, Cl^-, I^-, SCN^- and AcO^- in the form of their TBA salts. Only the addition of the F^- ions lead to significant changes in absorption band at 448 nm, which gradually disappeared while two new absorption bands at 538 nm and 342 nm appeared. These new absorption bands are attributable to an intramolecular charge transfer (ICT) transition. Simultaneously, quenching of the fluorescence resonance energy transfer (FRET) mediated emission at 535 nm was observed along with an enhancement in the fluorescence at 437 nm on treating compound **13** with F^- ions. Surprisingly, on addition of AcO^- ions to compound a gradual enhancement in the fluorescence at 437 nm was observed. In addition, the selectivity investigation of metal-ion binding for compound **13** was carried out with different ions, such as Na^+, K^+, Mg^{2+}, Ca^{2+}, Ag^+, Cd^{2+}, Ni^{2+}, Pb^{2+}, Cu^{2+}, Hg^{2+} and Co^{2+}, in acetonitrile and it was found to be highly selective toward Hg^{2+} among all the other metal ions.

Upon adding Hg^{2+} ions to solution of compound **13** a gradual fluorescence quenching owing to the formation of a ground state non-fluorescent complex was observed. These variations in the fluorescence were utilised to develop different logic circuits such as OR, XNOR and INH. Initially, the addition of F^- ions and Hg^{2+} ions provided the inputs (Inputs 1 and 2, respectively) to get output signals, which were recorded at 530 nm (Output 1) and at 430 nm (Output 2) to obtain XNOR and INH logic gates, respectively.

An additional logic gate has been developed using the fluorescence quenching of compound upon adding F^- and AcO^- ions. By employing fluorescence signals exhibited by compound **13** as an output on two chemical inputs (F^- and AcO^- ions) an OR logic gate was mimicked.

The anthraquinone and benzimidazole fused molecular entity **14** has been synthesised for multifunctional molecular logic circuits.[85] Among various anions, addition of F^- ions affected the UV/Vis spectrum of compound **14** along with a change in colour from yellow to orange. Along with the anions, the chemosensing properties of probe **14** towards various metal ions displayed red-shifted absorption bands only in the presence of Cu^{2+} and Zn^{2+} ions. On addition of Cu^{2+} ions to **14**, a colour change from yellow to purple was observed. On the other hand, on adding Zn^{2+} ions, a colour change from yellow to magenta was detected. Thus, the addition of different cations and anion as inputs has been used to obtain different output signals for logic gate applications. Initially, output signals were recorded at 465 nm and 495 nm to obtain INH logic and a XOR gate, respectively. These logic functions lead to molecular half-subtractor in which the XOR gate output was assigned the difference digit (D) and the INH gate the borrow digit (B) (Figure 20). In addition, the absorption output at 610 nm was monitored as it correlates with AND logic function (Table 8). These observations lead to molecular half-adder (Figure 20).

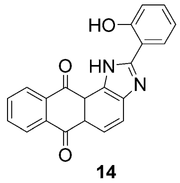

14

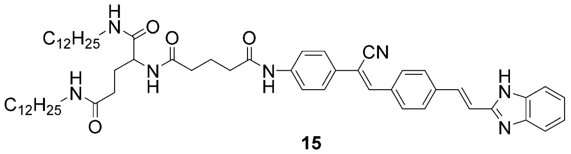

15

Table 8. Truth table for the operation of a half-adder and a half-subtractor.

Input 1 (F^-)	Input 2 (Cu^{2+})	Output (465 nm) INH	Output (495 nm) XOR	Output (610 nm) AND
0	0	0	0	0
0	1	0	1	0
1	0	1	1	0
1	1	0	0	1

When the chemical input was switched from Cu^{2+} to Zn^{2+}, to get different logic gates, half-subtractor and comparator gates were obtained. The absorption spectra have been recorded at 465 nm, 495 nm and 400 nm to get the output signals (Table 9) corresponding to INH, XOR and XNOR logic gates (Figure 21).

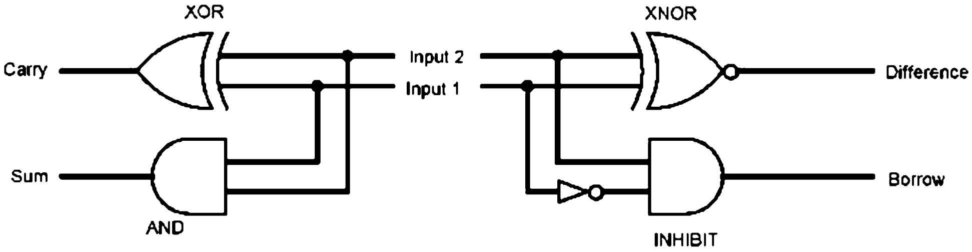

Figure 20. Logic circuit corresponding to a half-adder and a half-subtractor.

Table 9. Truth table for the operation of a comparator.

Input 1 (F^-)	Input 2 (Zn^{2+})	Output (465 nm) INH	Output (495 nm) XOR	Output (610 nm) XNOR
0	0	0	0	1
0	1	1	1	0
1	0	0	1	0
1	1	0	0	1

Table 10. Truth table compiled with different inputs.

Input 1 (H^+)	Input 2 (F^-/OH^-)	Input 3 excitation (400 nm)	Output emission (470 nm)
0	0	0	0
1	0	0	0
0	1	0	0
0	0	1	1
1	1	0	0
1	0	1	0
0	1	1	0
1	1	1	1

A novel gelator **15** consisting of one benzimidazole moiety and four amide units has been synthesised and used as a chemosensor for F^- ions.[86] Upon treating the receptor solution with different anions it displayed a significant colour change from yellow to red with F^- and OH^- ions. Thus, the UV/Vis output of the receptor solution represented a YES logic gate at 500 nm. The process of colour change was completely reversible on treating receptor:F^-/OH^- with trifluoroacetic acid (TFA). This can be implemented to the logic gate application to obtain a truth table by compiling UV/Vis outputs at 500 nm, and which corresponds to INH logic circuit.

Further, a combination gate of XNOR and AND with an emission output at 470 nm by input signals as addition of H^+, F^-/OH^- and excitation at 400 nm (Inputs 1, 2 and 3, respectively) has been obtained (Table 10 and Figure 22).

The receptor **15** formed a gel upon heating in DMSO followed by the addition of H_2O (20%; v/v). The gel thus formed was ion responsive and upon addition of OH^- ions, a phase transfer from gel to sol along with a distinguishable colour change from yellow to orange was observed. This resulted in the disappearance of the peak at 360 nm in the gel and the appearance of a peak at 424 nm in solution. In addition, an emission band of the gel at 540 nm shifted to 623 nm of solution. Similarly, the orange solution was changed back into yellow gel by adding TFA (Figure 23) and in excess of TFA, the gel phase not being destroyed, the emission band was gradually shifted to 570 nm.

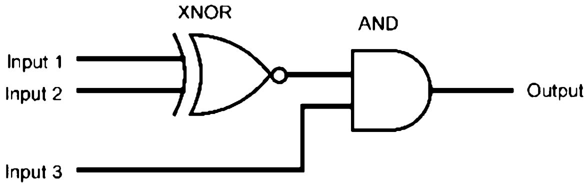

Figure 22. Combination logic circuit of XNOR and AND gates.

Based on these results, a more-complex logic gate with three inputs and three outputs was established. The addition of OH^- ions, H^+ ions and light (excitation at 400 nm) provided Inputs 1, 2 and 3, respectively. The emissions at 650 nm and absorbance at 450 nm were considered as Outputs 1 and 2, respectively (Table 11). A high value was given as the “1” state and the low value as the “0” state. The Output 1 first represented a XOR gate, which was activated by Input 3 to obtain

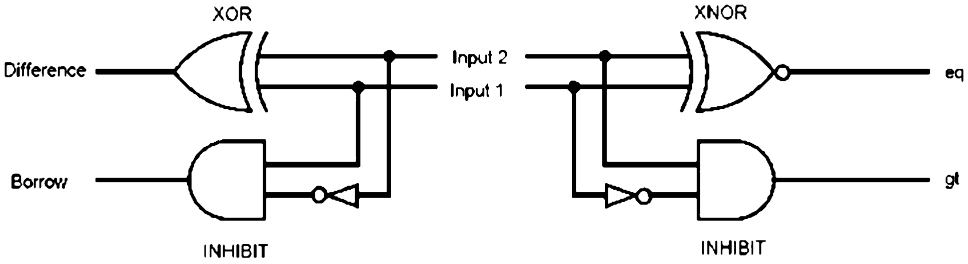

Figure 21. Logic circuit corresponding to operation of a comparator.

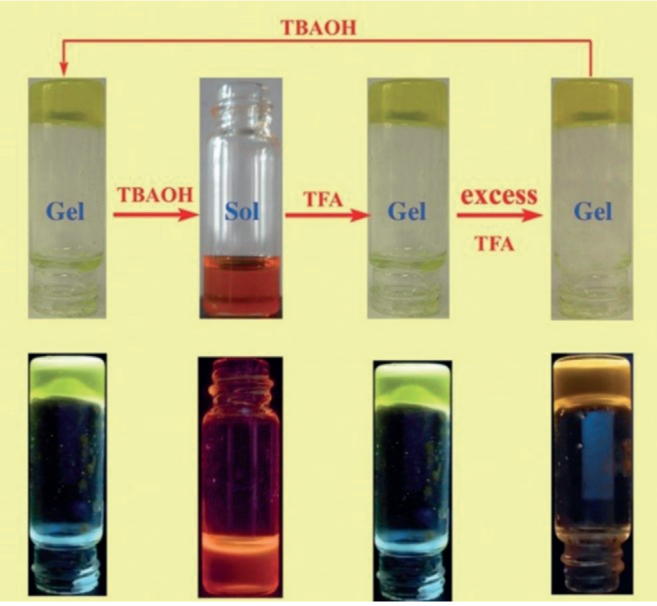

Figure 23. Photographs of compound **15** in DMSO/H_2O, which shows the responses to TBAOH and TFA (2 equiv); the upper row is in natural light, the bottom row is under illumination at 365 nm (reproduced from reference [86] with permission of Wiley-VCH).

Table 11. Truth table established with different inputs to obtain output signals for different logic gates.

Input 1 (OH^-)	Input 2 (H^+)	Input 3 excitation (400 nm)	Output 1 emission (650 nm)	Output 2 absorbance (450 nm)	Output 3 sol-gel state
0	0	0	0	0	1
1	0	0	0	1	0
0	1	0	0	0	1
0	0	1	0	0	1
1	1	0	0	0	1
1	0	1	1	1	0
0	1	1	1	0	1
1	1	1	0	0	1

another AND logic gate. The optical Output 2 built an INH logic gate. The Output 3 was created by the "sol–gel" state. The "gel" was considered as the "1" state whereas the "sol" was taken as the "0" state to obtain an exclusive-INH logic gate, which is a reverse signal to an INH logic gate (Figure 24).

Similar studies were carried out using F^- as the anion source; these investigations gave similar results and logic gates.

A colourimetric anion sensor **16**, based on dinitrophenyl hydrazone, was developed and its anion-sensing properties were investigated in DMSO.[87] Among the various anions tested, only AcO^-, $H_2PO_4^-$ and F^- displayed a significant change in the UV/Vis spectra as well as in colour (from yellow to pink). A deprotonation mechanism was proposed for the colourimetric detection process. Complete reversibility of this deprotonation process was achieved by adding cations, such as Zn^{2+} (Figure 25).

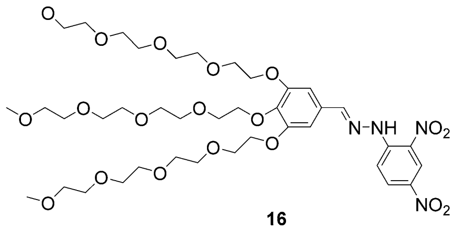

16

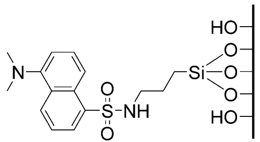

17

The reversible protonation/deprotonation property of **16** was further utilised for logic gate operations. For the detailed investigation of logic gate operations, addition of F^- ions and

Figure 25. Colour changes of sensor **16** in DMSO. Left to right: in the absence of ions, in presence of F^- ions and in presence of F^- ions and cation (see text for details; reproduced from reference [87] with permission of Wiley-VCH).

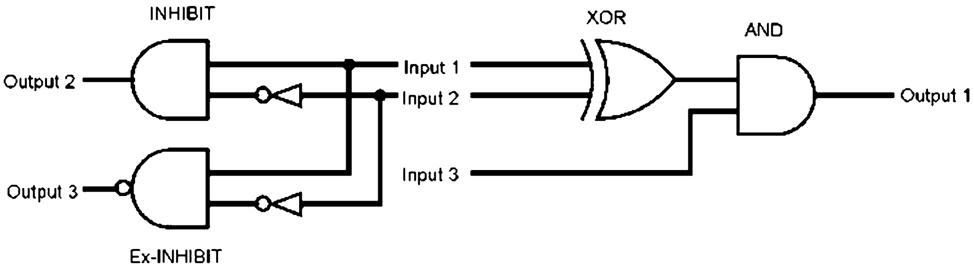

Figure 24. Complex logic circuit with three inputs and three outputs.

Zn^{2+} ions provided Inputs 1 and 2, respectively. The changes in absorbance at 407 nm and 498 nm were taken as Outputs 1 and 2, respectively. With various combinations of both inputs, the output signals corresponding to IMP and INH gates were obtained.

An SBA-15 (mesoporous silica)-based compound **17** (DA-SBA-15) has been synthesised and evaluated for the binding and detection of Hg^{2+} ions.[88] The fluorescence response of compound **17** towards various metal ions was investigated, in which Hg^{2+} ions induced progressive fluorescence quenching with increasing concentration. This fluorescence quenching was associated with the charge transfer within compound **17** and Hg^{2+} ions. Further, the effect of different anions on the fluorescence of compound **17** was investigated. In general the change in fluorescence on adding anions was much less; however, the presence of Cl^- or Br^- effectively eliminated the fluorescence quenching by Hg^{2+}. This property of compound **17** was utilised to establish a molecular logic gate. The change in fluorescence intensity of compound **17** in presence of metal ions and anions has been explained in three ways: 1) fluorescence quenching of the compound cannot occur in the absence of Hg^{2+} and in presence of Cl^- or Br^- (YES gate); 2) fluorescence quenching can occur in presence of Hg^{2+} in the absence of Cl^- or Br^- (NOT gate); 3) Cl^- or Br^- effectively eliminate fluorescence quenching by Hg^{2+} (AND gate). Thus, an INH logic gate was established by using output signals obtained from the addition of Hg^{2+} and Cl^- (or Br^-) as the two inputs. The change in fluorescence intensity at 510 nm was recorded as the output signal, which represented a circuit corresponding to an INH logic gate.

A Schiff base of naphthyl derivative **18** has been synthesised and investigated as a dual-ion receptor for Cu^{2+} ions and F^- ions.[89] The compound **18** showed characteristic absorption spectra at 385 nm attributed to charge transfer. UV/Vis titration of compound **18** with a various anions confirmed the selective recognition of F^- ions. Upon addition of TBAF to compound **18**, a new band at 460 nm with a significant colour change from yellow to red was observed (Figure 26). Compound **18** contains a 1,2-diamine chelating site and thus, its binding with heavy-transition-metal ions was examined; this revealed that compound **18** interacts selectively with Cu^{2+} ions. Incremental addition of Cu^{2+} ions resulted in a significant colour change from yellow to blue (Figure 26).

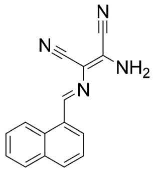

18

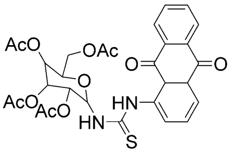

19

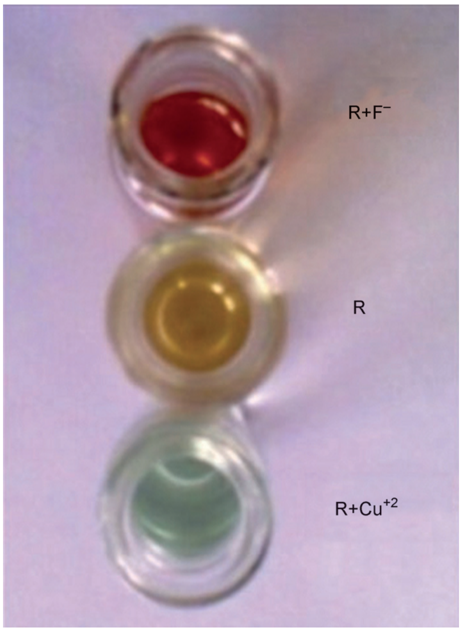

Figure 26. Visual changes of **18** with Cu^{2+} and F^- (reproduced from reference [89] with permission from the RSC).

Simultaneously, a gradual decrease in absorption at 385 nm with the appearance of a new broad band at 303 nm was observed. Further, in presence of either Cu^{2+} ions or F^- ions in a solution of compound **18** in dry tetrahydrofuran lead to strong emission at 430 nm. These results were utilised to obtain a logic gate circuit. The addition of F^- ions and Cu^{2+} ions provided the input signals (Inputs 1 and 2) and the changes in absorbance at 303 nm (A_{303}), 385 nm (A_{385}), 460 nm (A_{460}) and emission at 430 nm (F_{430}) were recorded as output signals (Table 12). Thus, the recognition behaviour of compound **18** demonstrates logic operations corresponding to OR, NOR, YES and INH functions with the addition of ions (Figure 27).

Table 12. Truth table for computation of logical functions with different chemical inputs.

Input 1 (F^-)	Input 2 (Cu^{2+})	Output 1 ($A_{303\,nm}$) YES	Output 2 ($A_{385\,nm}$) NOR	Output 3 ($A_{460\,nm}$) INH	Output 4 ($F_{430\,nm}$) OR
0	1	1	0	0	1
1	1	1	0	0	1
1	0	0	0	1	1
0	0	0	1	0	0

A thiourea-based peracetylated glucopyranosylanthraquinone conjugate **19** has been synthesised and its binding properties with different anions have been studied.[90] A distinct colour change from yellow to pink-red, owing to the deprotonation of the thiourea unit, was observed only on the addition of F^- ions, as well as a significant change in the fluorescence intensity. These processes of colour and fluorescence change were reversible upon treating with $Ca(ClO_4)_2$. These reversible reactions of compound **19** were investigated over four cycles of titrations carried out with addition of F^- ions (pink-red) and $Ca(ClO_4)_2$ (light yellow). Furthermore, the addition of F^- ions to

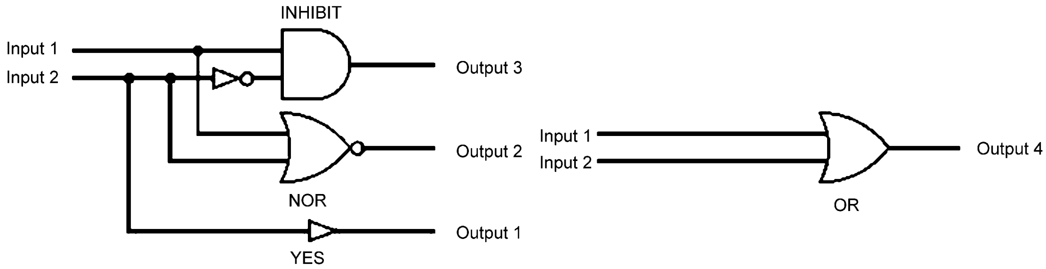

Figure 27. Representation of combinatorial circuit for YES, INH and NOR gates in absorption mode and OR gate in emission mode.

compound **19** displayed a remarkable fluorescence enhancement to show "ON" behaviour and the titration of this complex with $Ca(ClO_4)_2$ resulted in quenching of fluorescence intensity to act as an "OFF" switch. This repeated ON/OFF behaviour was utilised in molecular logic gate applications. The addition of F^- ions and $Ca(ClO_4)_2$ to compound **19** provided the input signals (Inputs 1 and 2) and the change in fluorescence intensity at 540 nm was taken as the output signal. Upon providing different input signals, an output signal corresponding to an INH logic gate was obtained.

A sensor **20**, which displayed strong emission selectively for AcO^- ions, has been synthesised by reacting 8-aminoquinoline with 2-hydroxy-1-naphthaldehyde.[91] The selective binding was attributed to the Y-shape of AcO^- ion, which was involved in double hydrogen-bond formation with the –OH and –CH=N– functionalities of sensor **20**. This binding leads to significant enhancement in emission spectra of sensor **20** and has been ascribed to twisted intramolecular charge transfer (TICT)-intramolecular charge transfer (ICT) state change. The binding ability of AcO^- to H^+ to form acetic acid (CH_3COOH) was utilised to investigate the change in fluorescence behaviour of sensor **20**. The "ON" state was achieved by adding AcO^- ions to sensor **20** in DMSO, upon which fluorescence enhancement was observed; the addition of H^+ ions to resulting solution lead to an "OFF" state (recovery of fluorescence intensity). This "OFF–ON–OFF" switching process was repeated several times with little loss of the fluorescent efficiency and it was further utilised to develop a logic gate operation with AcO^- and H^+ ions as two inputs. The change in fluorescence intensity at 520 nm was taken as the output signal. A truth table with these two inputs and output signal is given in Table 13, which results in an XNOR logic gate (Figure 28).

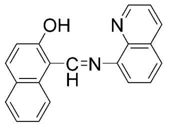

20

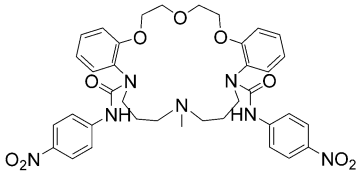

21

Table 13. Truth table for a XNOR logic gate.

Input 1 (AcO^-)	Input 2 (H^+)	Output (520 nm) XNOR
0	1	0
0	0	0
1	0	1
1	1	0

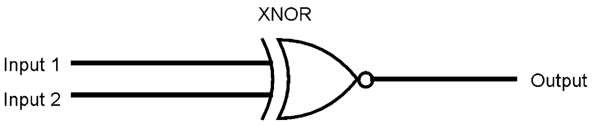

Figure 28. An exclusive-NOR (XNOR) logic gate formed with two chemical input systems.

Novel macrocyclic molecular probe **21**, which contains two nitrophenylurea moieties, has been synthesized; it was found to be active for the sensing of different anions (OH^-, F^- and CN^- ions).[92] In addition, the sensing reaction could be reversed by the addition of metal ions, such as Cu^{2+} or Hg^{2+} ions. This reversibility was used to develop logic gate. The addition of F^- ions and Cu^{2+} ions provided the inputs (Inputs 1 and 2, respectively) and the change in absorbance at 492 nm was considered as the output. The state "1" was defined if the absorbance at 492 nm was greater than 0.5 and state "0" if it was less than 0.5. In the absence of the two inputs, the output was as low as 0.014, which corresponds to the "0" state; in presence of F^- ions the absorbance was greater than 0.5, thus representing "1" state. The outputs of these inputs can be compiled in truth table that represents an IFNOT (INH) logic operation.

A receptor **22**, based on hexaphenylbenzene, that forms a spherical aggregation in aqueous media has been synthesised.[93] The receptor **22** is fluorescent in nature due to its aggregation-induced emission-enhancing characteristics and showed a ratiometric selective response for CN^- ions. The mechanism of ratiometric detection involved nucleophilic addition of CN^- ions, which disaggregated the spherical aggregation to form smaller nano aggregations. This disaggregation (formation of **22**:CN^- adduct) resulted in a visible colour change from colourless to yellow, with a significant change in absorption spectra and substantial changes in the emission spectra when excited at 282 nm. Under strong acidic condi-

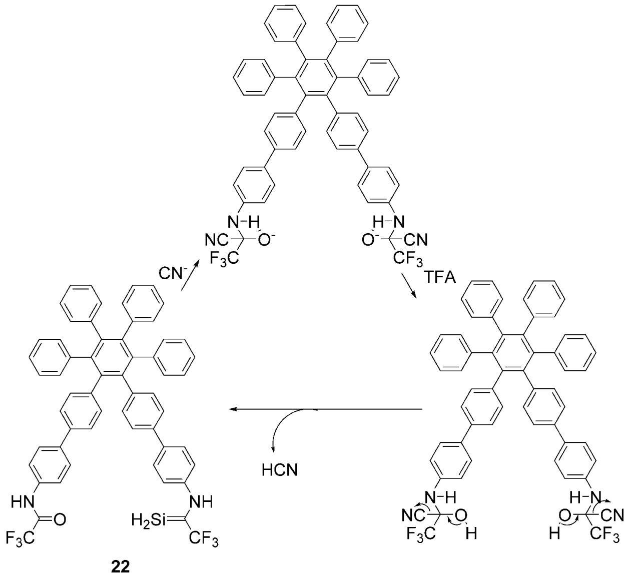

Figure 29. Probable reaction mechanism of detection.

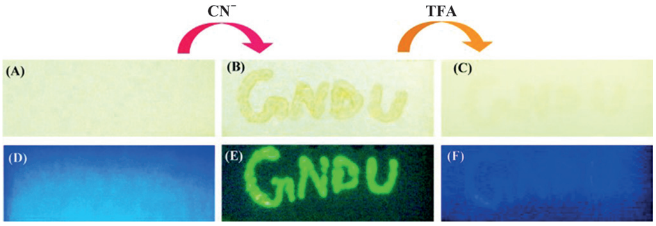

Figure 30. A)–C) Photographs of colour change and D)–F) photographs of fluorescence change under the UV lamp at 365 nm, of paper strips coated with chemosensor **22** in response to CN^- ions (reproduced from reference [93] with permission from the ACS).

tions, the reverse reaction of **22**:CN^- adduct was observed (Figure 29), which resulted in the restoration of colour as well as fluorescence quenching (Figure 30).

The reversibility was used to establish a logic circuit and “memory element” depending on the output signals as the emission changes at 380 nm and 485 nm (Outputs 1 and 2) with CN^- and TFA/H^+ as different chemical inputs (Inputs 1 and 2). Fluorescence intensities above the author specified threshold values (i.e., 150 a.u. for 380 nm and 90 a.u. for 485 nm) were assigned as the “1” state and below the threshold values as the “0” state. A logic circuit with two inputs and two outputs was constructed. The truth table (Table 14) discloses several combinations of inputs for “Output 1” and the sequential logic circuit of “Output 1” representing the set/reset element, which corresponds to the memory device. The reversible arrangements of set/reset logic operations is in a feedback loop and represents the memory feature with “”write–read–erase–read′“ functions through the output signals at 485 and 380 nm (Figure 31). Further, the write–erase cycles were demonstrated for receptor **22** through ″0–1“ states of fluorescence intensity by adding CN^- and TFA/H^+ alternately.

Table 14. Truth table for a sequential logic circuit.

Input 1 (CN^-)	Input 2 (H^+)	Output 1 (380 nm)	Output 2 (485 nm)
0	0	0	0
1	0	0	1
0	1	1	0
1	1	1	0
1	1	0	1

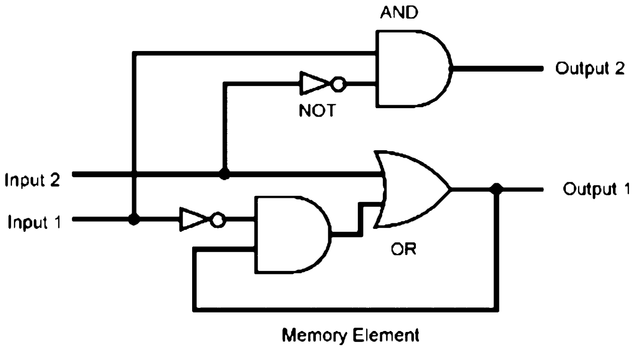

Figure 31. Sequential logic circuit displaying memory units with two inputs and two outputs.

Trivedi et al. designed and synthesised receptor **23** for the colourimetric detection of F^- and Cu^{2+} ions.[63] Upon treating receptor **23** with F^- ions, the colour changed from pale yellow to blue in DMSO and pale yellow to pink in MeCN. In addition, receptor **23** was able to detect Cu^{2+} ions with a colour change from pale yellow to orange-red. Adding Cu^{2+} ions to the receptor **23**:F^- ion complex resulted in the vanishing of the pink colour along with restoration of original pale yellow colour of receptor **23** (Figure 32b) The reversion process was evidenced by UV/Vis spectroscopy, in which the absorption band at 511 nm disappeared and the absorption band at 375 nm corresponding to receptor **23** was restored (Figure 32a). The mechanism for this restoration is given in Figure 33.

The switching operation of receptor **23** was further applied for a molecular logic gate in which the output signals (change in colour) were controlled by input signals (addition of F^- and Cu^{2+} ions). Thus, output signals in the form of spectral change at 511 nm were observed upon supplying two input signals as addition of F^- ions and Cu^{2+} ions; these changes signify an INH logic gate.

A simple chemosensor **24**, based on ferrocenedimalenonitrile, for selective and colourimetric detection of fluoride ions

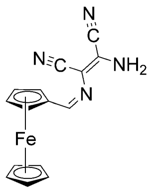

24

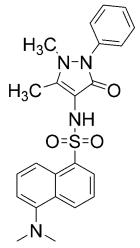

25

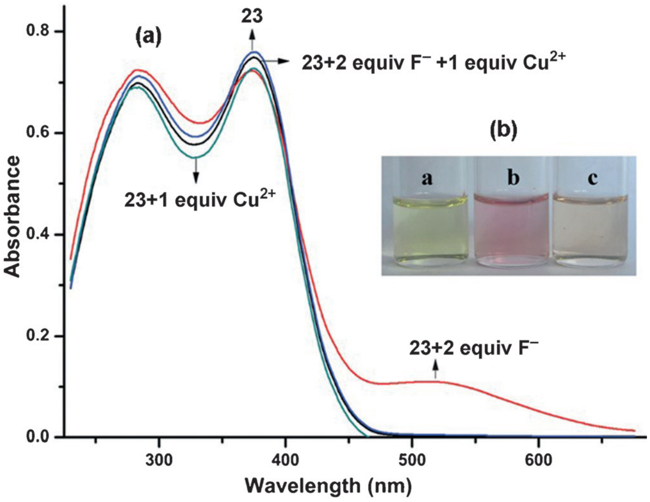

Figure 32. a) Reversal of the UV/Vis spectral pattern of receptor **23**+F^- upon the addition of Cu^{2+} ions. b) Corresponding colour changes in MeCN (reproduced from refreference [63] with permission from the RSC).

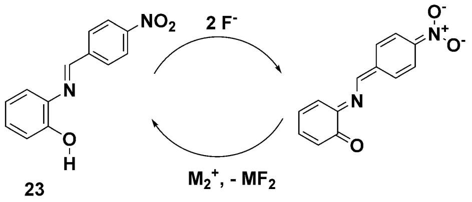

Figure 33. Reversal process of **23** upon addition of Cu^{2+} to the **23**+F^- in MeCN.

has been synthesised.[94] The chemosensor **24** was treated with various anions in the form of their TBA salts, upon which a significant colour change from red to orange-yellow was observed (Figure 34).

Receptor **24** also contains a 1,2-diamine chelating site, which is known to bind with Cu^{2+} ions, and thus the receptor was also investigated for the binding of Cu^{2+} ions. On the basis of this dual ion binding mechanism, the receptor was investigated for the logic gate functions. The addition of F^- and Cu^{2+} ions provided Inputs 1 and 2, respectively, and the changes in absorbance at 290 nm, 366 nm and 406 nm as Outputs 1, 2 and 3, respectively. The outputs are compiled in a truth table (Table 15) corresponding to YES, NOR and INH gates.

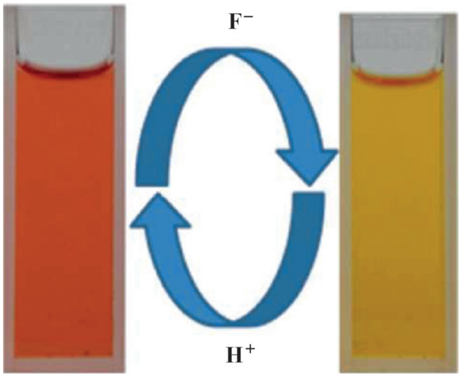

Figure 34. Visible colourimetric changes with fluoride and reversibility (reproduced from reference [94] with permission from the RSC).

Table 15. Truth table for different logic functions with various chemical inputs.

Input 1 (F^-)	Input 2 (Cu^{2+})	Output 1 (290 nm) YES	Output 2 (366 nm) NOR	Output 3 (406 nm) INH
0	1	1	0	0
1	1	1	0	0
1	0	0	0	1
0	0	0	1	0

In addition, the reversibility of the colourimetric output induced by F^- ions was achieved by adding trifluoroacitic acid (TFA) and the switching behaviour of receptor **24** wasinvestigated by alternate addition of H^+ and F^- ions to demonstrate the "writing–reading–erasing–reading" behaviour of the receptor.

A dyad receptor **25** based on dansyl and antipyrine fluorophores has been synthesised and its photophysical behaviour towards various cations and anions investigated.[95] The investigation showed that the **25** selectively detected Cu^{2+} ions relative to other metal ions. On incremental addition of Cu^{2+} ions, a new absorption band at 465 nm appeared and the fluorescence intensity at 528 nm decreased. The mechanism for this quenching of fluorescence is shows in Figure 34. In addition, receptor **25** showed ratiometric fluorescence emission behaviour upon the addition of F^- ions. This fluorescence emission behaviour was due to hydrogen-bonding interactions that restricted the photoinduced electron transfer (PET) from dansyl to antipyrine group (Figure 35).

The dual detection properties of **25** were utilised to construct a molecular logic gate. The addition of F^- ions and Cu^{2+} ions provided Inputs 1 and 2, respectively, and the change in fluorescent emission at 528 nm was considered as the output. Upon addition of either F^- ions or Cu^{2+} ions, the fluorescent emission at 528 nm was quenched. Thus, the output information at 528 nm with two chemical inputs mimic the Boolean values that correspond to the exclusive-NOR (XNOR) logic gate.

A colourimetric and turn-on fluorescent sensor **26** based on 2-hydroxy-1-naphthaldehyde has been synthesised for the selective detection of F^- ions.[69] The sensor **26** was able to detect F^- ions with high sensitivity and selectivity in aqueous

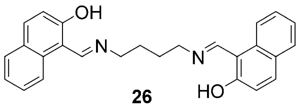

26

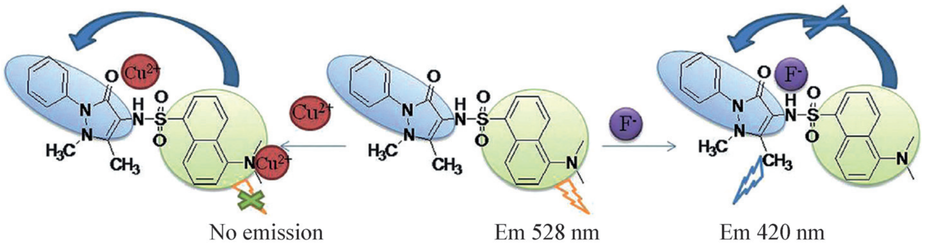

Figure 35. Proposed mechanism for binding of receptor with Cu^{2+} ions and F^- ions. (reproduced from reference [95] with permission from the RSC).

medium. This detection occurred as a result of hydrogen bond formation and deprotonation, which induced a colour change from pale yellow to deep yellow along with significant enhancement in the fluorescence. Upon the addition of H^+ ions to the sensor:F^- complex, the enhancement in fluorescence was restored to its original state (Figure 36). This reversibility can be expected as the deprotonated sensor is protonated on addition of H^+ ions.

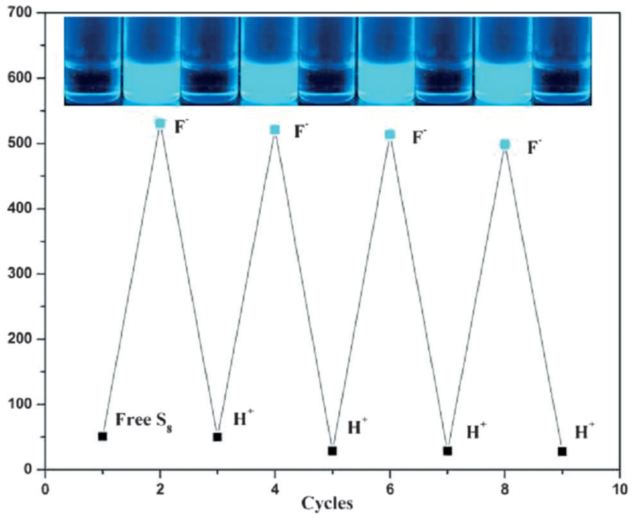

Figure 36. Reversibility study of **26** on adding F^- ions and H^+ ions (reproduced from reference [69] with permission from the RSC).

Further, this restoration process was utilised to establish a logic gate in which the addition of F^- ions and H^+ ions provided the input signals. The output signal was recorded with respect to change in fluorescence at 467 nm and represents an INH logic gate.

Sol–gel system based logic gates[86] can be used as electronic water purifiers because of their jellifying nature. Similarly they can also be used as pH monitoring equipment, since this system changes its physical nature with the change in pH. Hg^{2+} ions can be isolated by using a solid-supported Hg^{2+} ion sensing organic molecule.[88] On binding with an Hg^{2+} ion, the organic molecule displays significant change in colour, which is considered to be "ON" and more strong chelating agents (such as EDTA) can be introduced to make the system "OFF". Further, the logic gates that have switching properties[63,69,93,94] could be beneficial to develop memory switches, security keypads and molecular switches.

4. Cation–Anion Input Logic Gates

In this section logic gates are described based on the use of different chemical inputs in which addition of the cation is used as Input 1 and addition of the anion is used as Input 2.

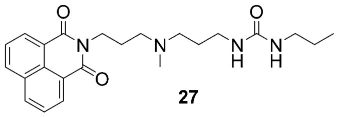

27

Compound **27**, containing a 1,8-naphthalimide fluorophore coupled with amine and urea receptor units, has been synthesised.[96] It was designed in such a way that it has a fluorophore–spacer–receptor1–spacer–receptor2 (Figure 37) conjugate such that a proton can bind at receptor1 (tertiary amine) and an anion can bind at receptor2 (urea subunit).

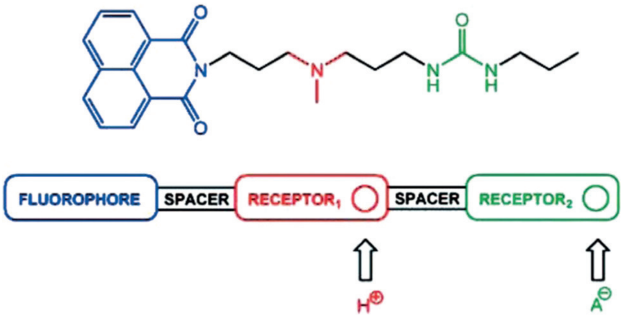

Figure 37. Fluorophore–spacer–receptor1–spacer–receptor2 system with proton (H^+) and anion (A^-) binding sites (reproduced from reference [96] with permission from the ACS).

Upon excitation at 325 nm, the unprotonated compound allows photoinduced electron transfer (PET), which results in the weak fluorescence. However, in presence of trifluoroacetic acid (TFA) as the proton source, the blocking of PET due to protonation of the tertiary amino function was observed and this resulted in the enhancement of fluorescence. Upon the addition of anions (F^-, AcO^- and $H_2PO_4^-$ ion) to the protonat-

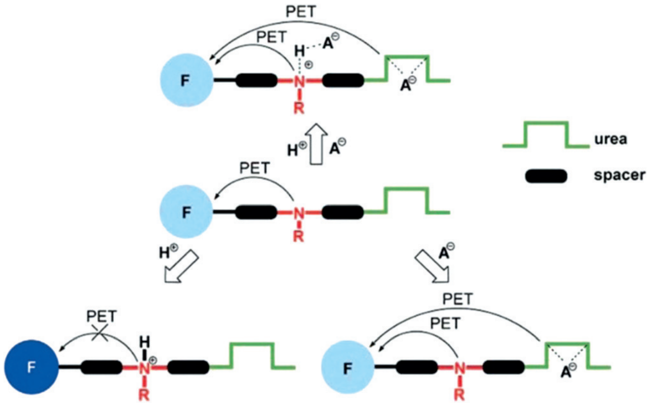

Figure 38. PET behaviour of compound **27** with addition of protons (H^+) and anions (A^-) (reproduced from reference [96] with permission from the ACS).

ed compound the fluorescence quenching owing to the reactivation of PET was observed (Figure 38).

The reversible behaviour of compound **27** was utilised to develop a molecular logic gate. The PET behaviour and thus change in fluorescence of compound **27** at 380 nm was recorded (Output) in the presence/absence of H^+ and anion (chemical inputs). The output values that were below a predefined threshold value were represented as the "0" state and above as the "1" state. The output signals obtained from different chemical inputs can be compiled in the truth table that corresponds to an INH logic gate.

A novel chemosensor **28** based on thiacalix[4]arene of 1,3-alternate conformation attached with pyrene has been synthesised.[97] This chemosensor demonstrated selective optical detection of Fe^{3+} and F^- ions in two complementary modes. In presence of Fe^{3+} ions, compound **28** displayed strong emission at 386 nm. In addition, when the compound was treated with various anions, it selectively detected F^- ions by quenching fluorescence. Thus, the chemosensor displayed an "ON–OFF" switching behaviour upon treatment with cations (Fe^{3+}) and anions (F^-). This "ON–OFF" switching behaviour was employed for logic gate applications with the change in emission at 386 nm as the output signal and the introduction of ions as the inputs. When the output signals are compiled in a truth table, the resulting circuit corresponds to a XNOR logic gate.

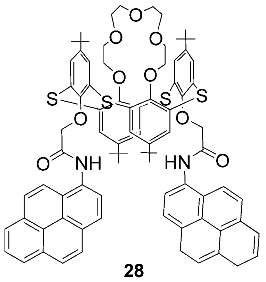

28

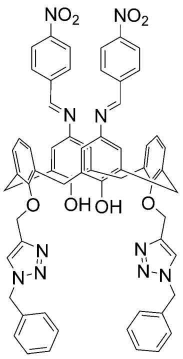

29

A bifunctional chromogenic calix[4]arene compound **29**, coupled with triazoles and hydroxyazophenols, has been synthesised for both cationic and anionic recognition.[98] Various metal salts were tested for the cationic binding properties of compound **29**. The compound is found to exhibit remarkable selectivity toward Ca^{2+}, Pb^{2+} and Ba^{2+} over other metal ions, as it contains metal-ligating triazole groups. The binding resulted in remarkable shift in absorption band from 390 nm to 496 nm (for Ca^{2+}), 501 nm (for Pb^{2+}) and 485 nm (for Ba^{2+}).

Upon treatment with Ca^{2+} ions in $MeCN/CHCl_3$ (v/v = 1000:4), the greenish solution of free compound **29** turned bright-yellow owing to the formation of a complex. In addition, compound **29** was able to specifically detect the F^- ions with a significant colour change from light green to bluish. As a result of this colour change, a remarkable shift in absorption band from 390 nm to 626 nm was observed. Consequently, the dual detection properties of compound **29** were employed to establish a logic gate circuit. In the absence of any chemical input, compound **29** displayed an absorption band at 390 nm and upon addition of Ca^{2+} or F^- ions, a bathochromic shift of the absorption band to 496 nm or 626 nm, respectively, was observed. However, no such absorption band at 626 nm was observed when F^- ions were added to a solution of compound **29**:Ca^{2+} complex in $MeCN/CHCl_3$ (v/v = 1000:4). This property of compound **29** provided a promising structure to mimic an INHIBIT logic gate along with a YES logic function. The addition of Ca^{2+} ions and F^- ions provided the chemical inputs (Inputs 1 and 2, respectively) and the changes in absorption bands at 496 nm and 626 nm were considered as output signals (Outputs 1 and 2, respectively) to obtain a truth table (Table 16) corresponding to INH and YES logic gates (Figure 39).

A new ninhydrin-based colourimetric molecular switch (receptor **30**) has been designed and synthesised by Upadhyay

Table 16. Truth table for YES and INH gates.

Input 1 (Ca^{2+})	Input 2 (F^-)	Output 1 (496 nm) YES	Output 2 (626 nm) INH
0	0	0	0
1	0	1	0
0	1	0	1
1	1	1	0

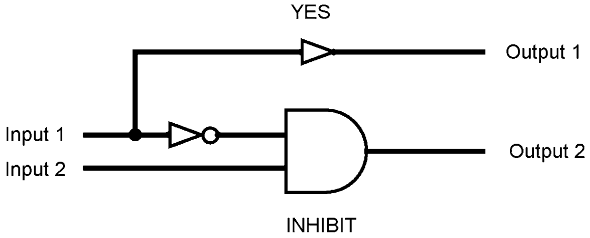

Figure 39. Logic circuit of combinational gate.

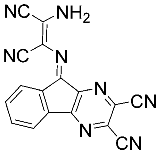

30

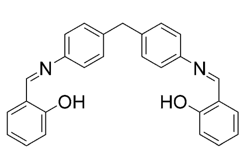

31

and co-workers.[99] No significant change was observed on the addition of various cations or anions separately to the receptor **30**. However, when the solution of receptor **30** in EtOH/H_2O containing CH_3COO^-/F^- was treated with various cations, addition of Hg^{2+} ions lead to a significant change in colour from purple to blue. Thus, the receptor **30** is switched "ON" (blue) in presence of Hg^{2+} and CH_3COO^-/F^- together and the absence either cation or anion switches the system to "OFF" (purple) mode. This unique property was applied for logic gate applications. The addition of Hg^{2+} and CH_3COO^-/F^- provided the chemical input signals (Inputs 1 and 2, respectively) and the absorbance change at 590 nm was designated as the output signal. The absorption change at 590 nm was compiled to obtain a truth table that represents an AND logic gate.

A dipodal sensor **31** has been synthesised by condensing salicylaldehyde with 4,4′-methylenedianiline; the sensor was able to detect Al^{3+} in HEPES buffered THF/H_2O (7:3, v/v).[100] The detection mechanism followed excited state proton transfer (ESPT), which resulted in a fluorescence quenching at 355 nm and fluorescence enhancement at 480 nm. The resulting aluminium complex (**31**:Al^{3+}) showed a high selectivity towards perchlorate ions over other anions tested. Upon treating the complex with perchlorate ions a new band at 428 nm emerged. This sensing property of **31** was utilised to develop logic gate. The addition of Al^{3+} and ClO_4^- provided the chemical inputs (Inputs 1 and 2) and the fluorescence change at 428 nm was considered as the output signal. The compilation of output signals satisfied the conditions corresponding to an AND molecular logic gate.

A novel and simple fluorescent chemosensor **32** based on rhodamine has been designed and synthesised for the detection of Hg^{2+} ions.[101] It displayed a very high selectivity and sensitivity with a detection limit at 10^{-8} M level for Hg^{2+} ions. Upon addition of Hg^{2+} ions to chemosensor **32** a significant colour change from colourless to pink was noted. The chemosensor showed a 400-fold enhancement in fluorescence emission intensity at 595 nm upon binding with Hg^{2+} in 50 % H_2O/CH_3CN HEPES buffer at pH 7.0. The reverse reaction was achieved by treating the chemosensor:Hg^{2+} complex with I^- ions. Simultaneously, the colour of the complex changed from pink to colourless and fluorescent emission intensity of the system at 595 nm was quenched, which indicates that the coordinated Hg^{2+} ions with the chemosensor were replaced by I^- ions. This reversibility was utilised to develop a logic gate; the addition of Hg^{2+} ions and I^- ions provided Inputa 1 and 2, respectively, to obtain an output signal in the form of change in emission intensity at 595 nm. The output signals can be tabulated to obtain a truth table (Table 17) corresponding to an INH logic gate.

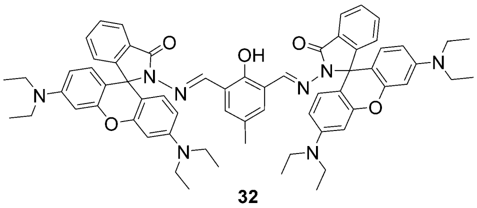

32

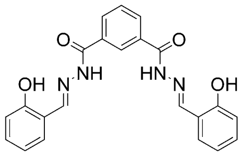

33

Table 17. Truth table for an INH logic gate with a two-input system.

Input 1 (Hg^{2+})	Input 2 (I^-)	Output (595 nm) INH
0	0	0
0	1	0
1	0	1
1	1	0

A simple receptor **33** that selectively detects Al^{3+} and pyrophosphate, PPi ($P_2O7_4^-$) has been synthesised by condensing isophthaloyl hydrazide with salicylaldehyde.[102] The change in photophysical properties of receptor **33** was tested by treating it with various metal ions such as Na^+, K^+, Ba^{2+}, Ga^{3+}, Mg^{2+}, Ca^{2+}, Mn^{2+}, Fe^{2+}, Ni^{2+}, Co^{2+}, Zn^{2+}, Cu^{2+}, Ag^+, Cd^{2+}, Hg^{2+}, Pb^{2+}, In^{3+}, Cr^{3+}, Fe^{3+} and Al^{3+}, as well as the several anions such as AcO^-, Cl^-, Br^-, I^-, F^-, BzO^-, SH^-, $H_2PO_4^-$, PO_4^{3-}, S^{2-}, N_3^-, $P_2O_7^{4-}$ and ADP in MeOH:H_2O (1:1, v/v) as their salts. However, enhancement in emission was observed only with the addition of Al^{3+} and $P_2O_7^{4-}$ ions and this was used to mimic logic gates. The addition of Al^3+ and $P_2O_7^{4-}$ ions provided the two chemical inputs (Inputs 1 and 2). The changes in fluorescence at 455 nm and 508 nm were considered as the output signals (Outputs 1 and 2, respectively). The output signals obtained by varying chemical inputs can be compiled to get a truth table that corresponds to an INH logic gate for both signals. These output signals can also be compiled together to obtain a new signal that represents an exclusive-OR (EXOR) logic gate (Figure 40). The truth table for EXOR logic gate is given in Table 18.

A chemosensor **34** based on thiacalix[4]arene attached to naphthyl group at 1,3-alternate conformations has been synthesised.[103] This chemosensor showed high selectivity toward CN^- ions over other anions such as F^-, Cl^-, Br^-, I^-, AcO^-, HSO_4^-, $H_2PO_4^-$ and NO_3^- by hydrogen bonding and a displacement approach. The addition of CN^- resulted in quenching of the fluorescence emission of compound **34**. Further, chemosensor **34** showed high selectivity for Fe^{3+} ions over other cat-

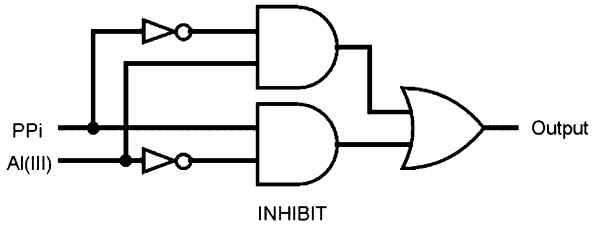

Figure 40. Logic of EXOR gate.

Table 18. Truth table of an exclusive-OR gate (EXOR gate).

Input 1 (Al^{3+})	Input 2 ($P_2O_7^{4-}$)	Output EXOR
0	0	0
1	0	1
0	1	1
1	1	0

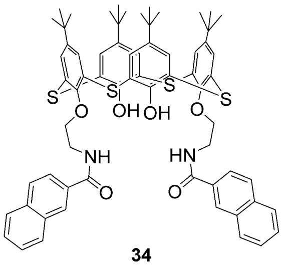

34

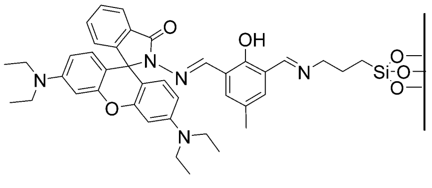

35

ions, such as Li^+, Na^+, Ba^{2+}, Mg^{2+}, Ni^{2+}, Cu^{2+}, Zn^{2+}, Cd^{2+}, Hg^{2+}, Ag^+, Pb^{2+}, Co^{2+}, Fe^{2+} and K^+, by quenching the fluorescence emission. Thus, depending upon the dual detection property of chemosensor **34**, a molecular computing logic gate has been developed. The addition of Fe^{3+} and CN^- ions provided the chemical inputs (Inputs 1 and 2, respectively) and the change in fluorescence emission at 350 nm was taken as the output signal; these results can be compiled in a truth table that corresponds to an exclusive-NOR (XNOR) logic gate.

Modified SBA-15 nanocomposite **35** with rhodamine group attached has been synthesised and investigated for Hg^{2+} ion detection.[104] In presence of Hg^{2+} ions a colourless solution of sensor **35** in $MeCN/H_2O$ solution (9:1 v/v) turned red. Further, the fluorescent detection limit for Hg^{2+} was at the 15 ppb level. The addition of Hg^{2+} to the solution of sensor caused fluorescence enhancement; however, on addition of S^{2-} to the mixture of Hg^{2+} and sensor solution, the fluorescence is turned off along with the restoration of colourless solution. This indicates that S^{2-} restricts the binding of Hg^{2+} ions to sensor **35**. A logic gate has been established using this reversibility. The addition of Hg^{2+} and S^{2-} to sensor **35** provided the inputs (Inputs 1 and 2, respectively) and the change in fluorescence intensity at 580 nm was taken as the output signal to obtain a logic function corresponding to an INH logic gate.

A rhodamine-based dual signalling compound **36** was synthesised for the optical detection of Hg^{2+} ions.[105] The compound displayed a 252-fold enhancement in the fluorescence at 553 nm in presence of Hg^{2+} ion; and the enhancement was completely reversible upon treating the compound **36**:Hg^{2+} complex with I^- ions (Figure 41).

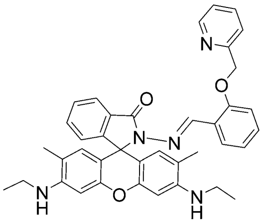

36

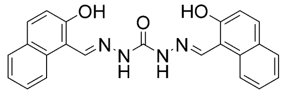

37

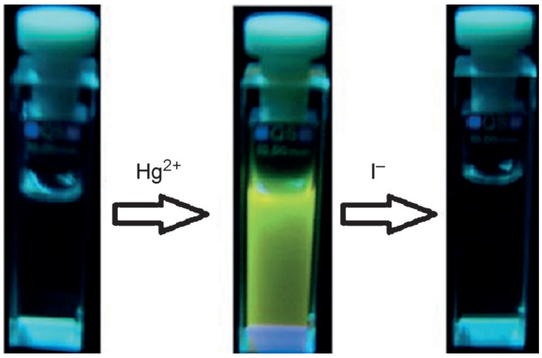

Figure 41. UV-exposed photographs of **36**, **36**:Hg^{2+} and **36**:$Hg^{2+}+I^-$ in $MeCN/H_2O$ solvent (reproduced from reference [105] with permission from Wiley-VCH).

The reversibility was utilised for a molecular computational system. The addition of Hg^{2+} and I^- provided the chemical inputs (Inputs 1 and 2) and the change in fluorescence emission at 553 nm was specified as output signal. The fluorescence enhancement was observed only in presence of Hg^{2+} ions and thus was designated by the Boolean value "1"; for all other inputs the enhancement in emission was not observed and thus given the Boolean value "0". From the overall output, a logic circuit corresponding to an INH logic function was obtained.

A simple organic receptor **37** has been synthesised by condensing 2-naphthol-1-aldehyde with thiourea.[106] The binding behaviour was investigated in $DMSO:H_2O$ (v/v = 9:1) by treating receptor **37** with different anions; only F^-, AcO^- and $H_2PO_4^-$ displayed a distinguishable optical response, that is, a significant change in the absorption spectra as well as in emission spectra was observed. Similarly, receptor **37** showed significant optical response upon adding Zn^{2+}, Cu^{2+}, Co^{2+} and Ni^{2+} ions along with measurable changes in absorbance and emission. In addition, the reverse reaction for receptor **37** has been investigated and verified by the introduction of Ca^{2+} (for F^{-}) and EDTA (for Zn^{2+}/Cu^{2+}) into the system. On the basis of above results, a two input logic gates have been developed. As shown in Figure 42, output signals were recorded as the changes in absorbance at 381 nm and 439 nm (Outputs 1 and 2, respectively) and the change in fluorescence at 520 nm (Output 3) upon the addition of Zn^{2+} and F^{-} ions as the inputs (Inputs 1 and 2, respectively). The output signals can be compiled to get a truth table (Table 19) that represents NOR and OR gates (Figure 43).

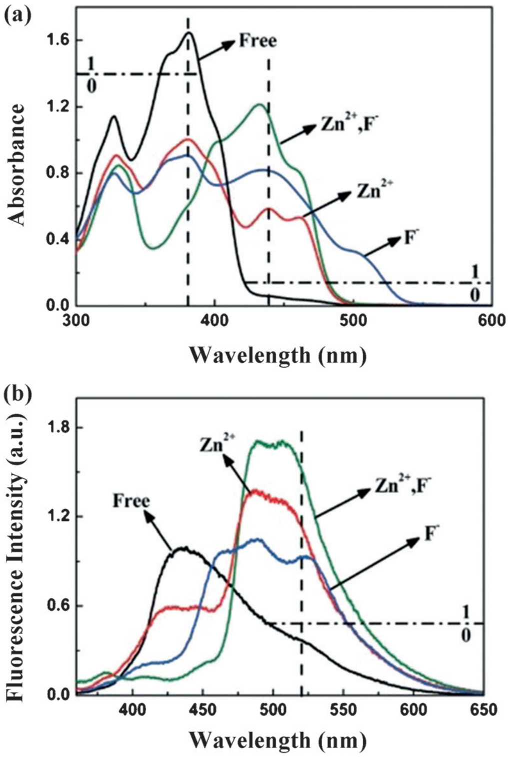

Figure 42. Change in a) absorption and b) fluorescence spectra of receptor **37** with the addition of Zn^{2+} (Input 1) and F^{-} ions (Input 2) (reproduced from reference [106] with permission from the RSC).

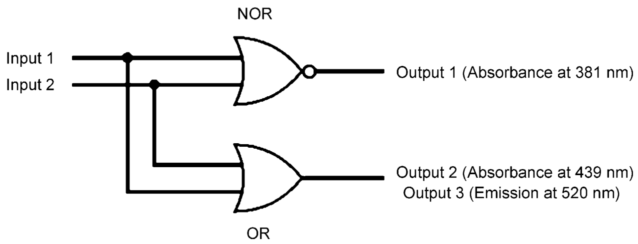

Figure 43. Logic circuit for the NOR/OR gates.

Further, addition Cu^{2+} was introduced as a third input (Input 3) to develop a complicated three-input system logic gate. The changes in absorption spectra and emission spectra are given in Figure 44. The changes in output signals with the addition of Cu^{2+} ions (Input 3) to the system have been compiled into a truth table (Table 20) to obtain a complicated logic gate (Figure 45).

Table 19. Truth table corresponding to NOR, OR and OR logic gates.

Input 1 (Zn^{2+})	Input 2 (F^{-})	Output 1 ($A_{381\,nm}$) NOR	Output 2 ($A_{439\,nm}$) OR	Output 3 ($F_{520\,nm}$) OR
0	0	1	0	0
1	0	0	1	1
0	1	0	1	1
1	1	0	1	1

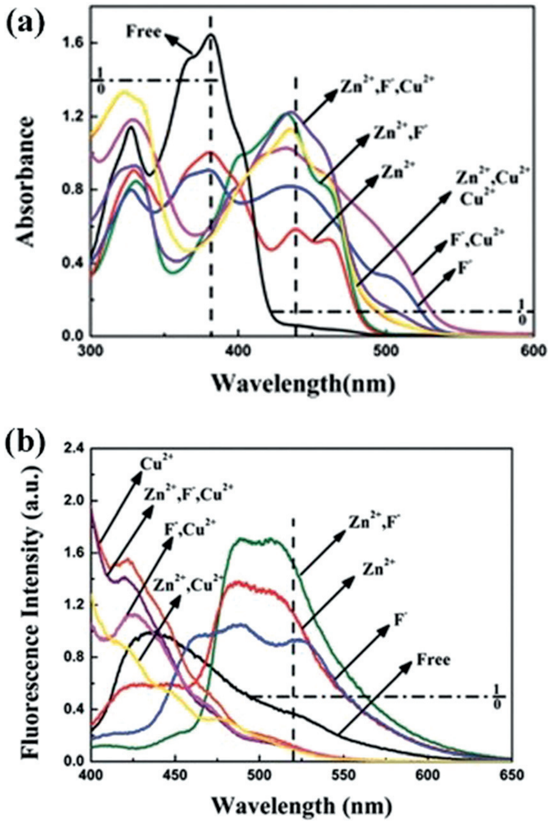

Figure 44. Change in a) absorption and b) fluorescence spectra of receptor **37** with the addition of Zn^{2+} (Input 1), F^{-} (Input 2) and Cu^{2+} (Input 3) ions (reproduced from reference [106] with permission from the RSC).

A benzothiazole functionalised chemosensor **38**, has been synthesised and investigated for both colourimetric and fluorometric responses by adding various metal ions; it was found that chemosensor **38** was selective towards Zn^{2+} and Cd^{2+} ions at physiological pH.[107] The addition of metal ions (Zn^{2+} or Cd^{2+} ions) leads to complex formation that inhibits PET and thus enhancement in fluorescence emission was observed. Further, these metal:chemosensor complexes were treated with various anions, among which the addition of pyrophosphate (PPi, $P_4O_7^{4-}$) and $H_2PO_4^{-}$ ions resulted in fluorescence quench-

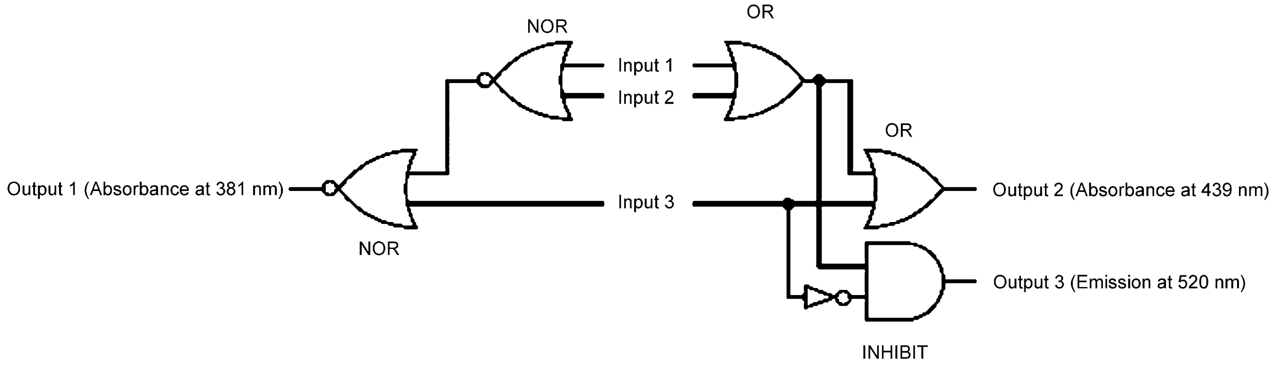

Figure 45. A three-input, three-output combinatorial molecular logic circuit.

Table 20. Truth table for a three-input situation.

Input 1 (Zn^{2+})	Input 2 (F^-)	Input 3 (Cu^{2+})	Output 1 ($A_{381\,nm}$) NOR	Output 2 ($A_{439\,nm}$) OR	Output 3 ($F_{520\,nm}$) INH
0	0	0	1	0	0
1	0	0	0	1	1
0	1	0	0	1	1
1	1	0	0	1	1
0	0	1	0	1	0
1	0	1	0	1	0
0	1	1	0	1	0
1	1	1	0	1	0

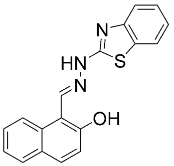

38

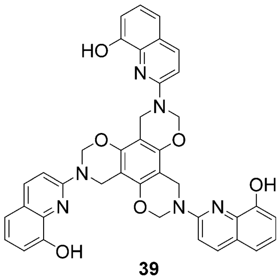

39

ing. The reverse reaction for chemosensor **38** was achieved by treating the Zn^{2+} complex with PPi ($P_4O_7^{4-}$) ions (Figure 46).

This reversible property was utilised to develop logic circuits. The addition of Zn^{2+} and pyrophosphate provided Inputs 1 and 2, respectively, to obtain output signals as a change in emission at 510 nm, which corresponds to INH logic gate.

A new C_3-symmetric tri-arm 8-hydroxyquinoline based fluorescent chemosensor **39** has been designed and synthesised for ratiometric and selective detection of Zn^{2+} over a wide range of metal ions.[108] The addition of Zn^{2+} to the chemosensor solution in organo-aqueous solvent was induced to give a 1:3 ligand–metal complex. The formation of **39**$\cdot 3\,Zn^{2+}$ resulted in a significant enhancement in the fluorescent emission spectra at 491 nm which was attributed to an internal charge transfer mechanism. In addition, the **39**$\cdot 3Zn^{2+}$ complex was a selective "turn-ON" fluorescent sensor for pyrophosphate (PPi) ion (Figure 47).

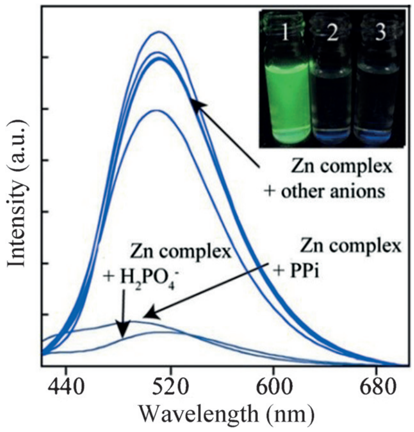

Figure 46. Change in fluorescence emission spectra of the **38**:Zn^{2+} ensemble upon addition of various anions. Inset: The visual change in fluorescence of 1) **38** 2) after adding $P_4O_7^{4-}$ and 3) $H_2PO_4^-$ ions (reproduced from reference [107] with permission from Elsevier).

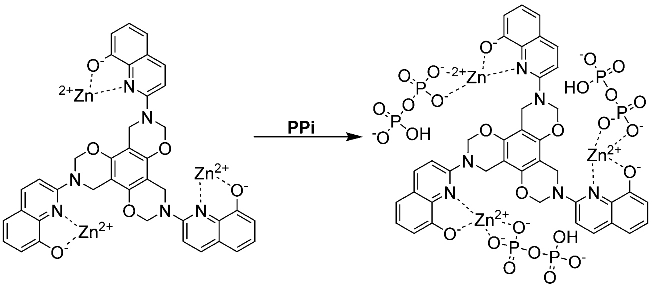

Figure 47. Binding mechanism of pyrophosphate to **39**.

This change in fluorescence was utilised to establish logic gate circuits. The addition of Zn^{2+} and PPi ($P_4O_7^{4-}$) provided the input signals (Inputs 1 and 2, respectively) and the changes in fluorescence emission at 491 nm and 453 nm were taken as Outputs 1 and 2, respectively (Table 21), lead to INHIBIT and AND logic gates, respectively (Figure 48).

A boron-dipyrrin based organic sensor **40** has been designed and synthesised to prepare coordination complexes of Hg^{2+} ions.[109] Upon addition of Hg^{2+} ions to a solution of **40** in CH_3CN/PBS (7:3; v/v, pH 7.4), a significant change in fluores-

Table 21. Truth table for a combinational logic gate.

Input 1 (Zn^{2+})	Input 2 ($P_4O_7^{4-}$)	Output 1 (491 nm) INH	Output 2 (453 nm) AND
0	0	0	0
1	0	1	0
0	1	0	0
1	1	0	1

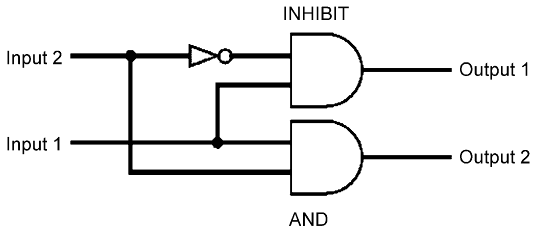

Figure 48. Combinational logic circuit.

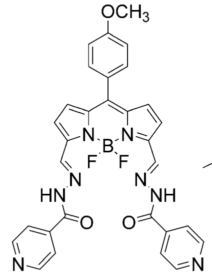

40

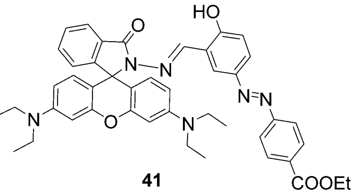

41

cence emission and absorbance was observed along with a change in fluorescent colour from highly red solutions under a UV lamp to non-fluorescent blue solutions (Figure 49a). Further, the **40**:Hg^{2+} complex can be used for the specific detection of Cl^- ions. The detection process involved restoration of original spectral values of sensor along with colour change from non-fluorescent blue solutions to highly red fluorescent solutions under a UV lamp (Figure 49b).

The reversible nature of **40** was applied to establish a molecular logic gate wherein **40** displayed switching properties with the introduction of Hg^{2+} ions and Cl^- ions (Figure 50). An IMP logic circuit was established with the help of this "ON–OFF" switching property. The addition of Hg^{2+} ions and Cl^- ions provided the inputs (Inputs 1 and 2) and the change in fluorescence emission at 615 nm was considered as the output signal, representing the IMP logic circuit.

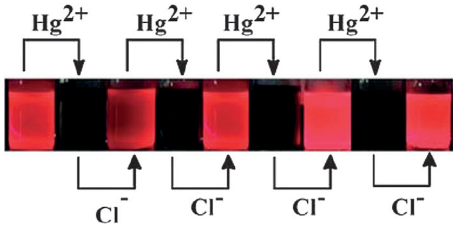

Figure 50. Switching properties of the sensor **40** with the addition of Hg^{2+} and Cl^- ions (reproduced from reference [109] with permission from the RSC).

Sensor **41** based on azo-rhodamine has been synthesised and can act as "OFF–ON" reversible luminescent probe for Sn^{4+} detection.[110] The sensor was selective only to Sn^{4+} ions over many other cations tested. The sensing behaviour of **41** was demonstrated by measuring the change in fluorescence, change in absorbance, and change in visual fluorescence. A significant visual colour change from pale yellow to pink only in the presence of Sn^{4+} ions was observed owing to spiro ring-opening. This ring opening also lead to a change in the emission colour of the sensor solution from dark to orange. The detection process was completely reversible upon addition of a counterion such as S^{2-}. The mechanism of spiro ring opening, reversibility and the changes in visual and emission colours are given in Figure 51.

The restoration properties of the sensor allowed the design of a molecular logic gate for which the addition of Sn^{4+} and S^{2-} provided the Inputs 1 and 2, respectively. The change in emission intensity at 582 nm was considered as the output signal. On addition of Sn^{4+} ions, the output showed good en-

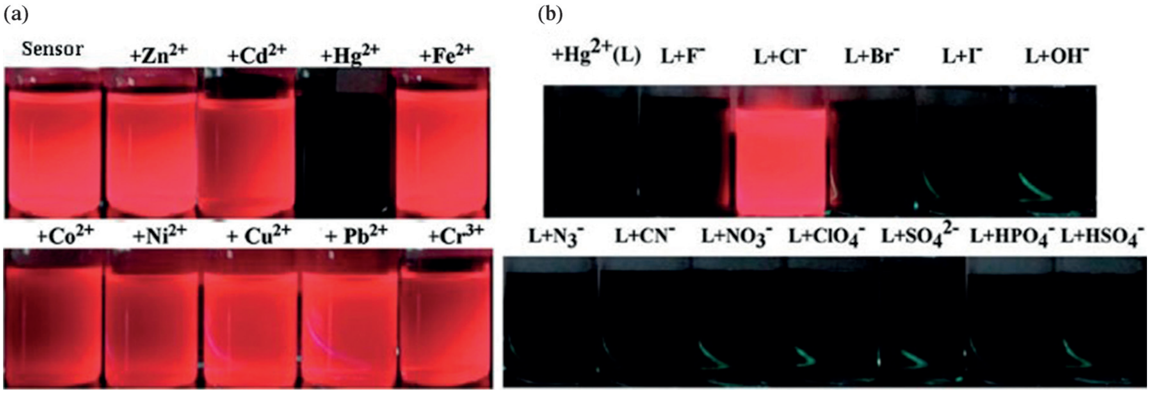

Figure 49. a) Change in colour upon adding various metal ions to **40** under a UV lamp; b) Change in colour upon adding various anions to the **40**:Hg^{2+} complex under a UV lamp (reproduced from reference [109] with permission from the RSC).

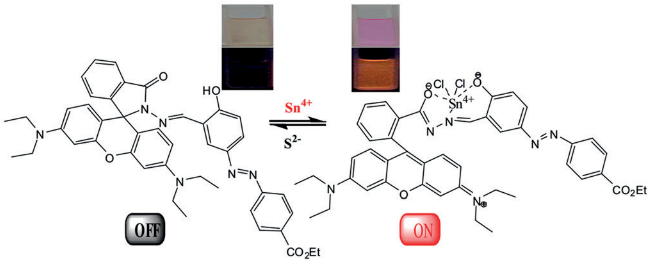

Figure 51. Change and reversibility of colour of **41** on adding ions and mechanism of binding as well as reversal process (reproduced from reference [110] with permission from the RSC).

Table 22. Truth table for an INH logic gate.

Input 1 (Sn^{4+})	Input 2 (S^{2-})	Output 1 (582 nm) INH
0	0	0
1	0	1
0	1	0
1	1	0

hancement in the emission intensity which, therefore, was considered as the Boolean value “1” and for all other inputs this value was “0”. The output signals are tabulated in Table 22, which represents an INH logic circuit.

An “ON–OFF–ON” type fluorescent receptor **42** containing benzimidazole group and hydroxyl functionality as binding unit has been developed.[111] The receptor exhibited high selectivity and sensitivity for Cu^{2+} ions over other cations. The significance of this receptor is that it was able to detect the Cu^{2+} ions in 100% aqueous solution. Receptor **42** displayed a strong absorbance at 329 nm which gradually decreased upon increasing concentration of Cu^{2+} (0–1 equiv). This indicated that the coordination of **42** to paramagnetic Cu^{2+} took place (Figure 53). Once combined with Cu^{2+}, the blue fluorescence of **42** was completely quenched due to the formation of **42**:Cu^{2+} complex. Further, this complex was screened for colourimetric detection of various anions and it was found that it selectively detected S^{2-} based on displacement approach (Figure 53). The mechanism of this detection process is given in Figure 52.

Thus, **42** behaved as an “ON–OFF” switch, based on two different fluorescence emission states. The receptor was analysed for a molecular logic gate application in which the addition of Cu^{2+} and S^{2-} ions provided the Inputs 1 and 2, respectively. The change in fluorescent emission was taken as the output. On addition of Cu^{2+} ions to a solution of **42** in HEPES-buffer (20 mM, pH 7.4), a 1:2 metal:ligand complex is formed. This binding quenches the fluorescence emission of **42**. Further, addition of S^{2-} to this complex leads to removal of coordination from the complex, making **42** free. Therefore, the fluorescence emission is restored. The addition of ions and fluorescence emission were considered as the Boolean operation “0”. The output of this logic gate represents an IMP operation.

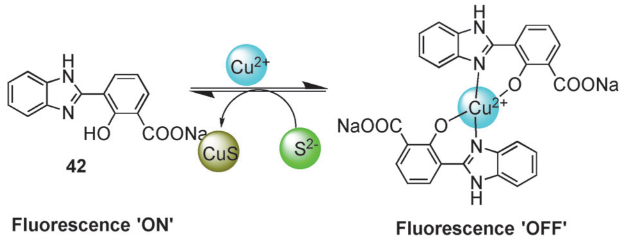

Figure 52. Binding mechanism of receptor **42**.

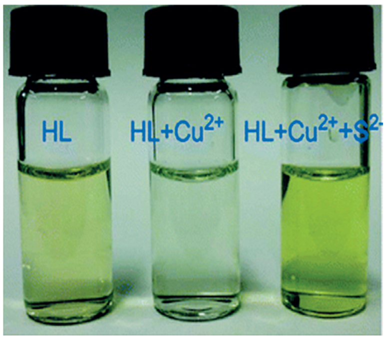

Figure 53. Colour change upon adding different ions to receptor **42** (reproduced from refreference [111] with permission from the RSC).

Chromophore **43** based on osmium(II) complex has been designed and synthesised.[29] The chromophore showed significant change in its UV/Vis spectra by chemical stimulation upon adding Cu^{2+} and F^- ions. The addition of Cu^{2+} ions to **43** lead to a bathochromic shift from 293 nm to 337 nm, associated with a remarkable “turn-OFF” change at 509 nm and 687 nm. Simultaneously, a colour change from light brown to colourless was recorded (Figure 54). This significant change was attributed to the formation of oxidative osmium (Os^{3+}) species. On the other hand, the addition of F^- displayed entirely different information and a significant bathochromic shift has been observed at 509 nm as well as shoulder at 325 nm along with a significant colour change from light brown to red in real time (Figure 54).

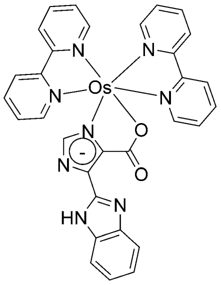

43

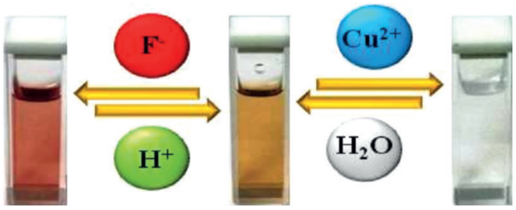

Figure 54. Colour change of **43** upon adding Cu^{2+} and F^- ions along with the reversal process (reproduced from reference [29] with permission from the RSC).

The detection of Cu^{2+} and F^- ions was deployed to develop several logic gates with different input–output systems. Initially the addition of Cu^{2+} was taken as Input 1 and addition of H_2O was considered as Input 2. The output signals were measured as the changes in absorbance at 509 nm and 293 nm, which were considered as Outputs 1 and 2, respectively (Table 23). Upon adding Cu^{2+} ions and H_2O in different combinations, the output signal at 509 nm represented an INH logic circuit and the output signal at 293 nm contributed an IMP logic circuit (Figure 55).

Table 23. Truth table for INH and IMP logic gates.

Input 1 (Cu^{2+})	Input 2 (H_2O)	Output 1 INH	Output 2 IMP
0	0	0	1
0	1	0	1
1	0	1	0
1	1	0	1

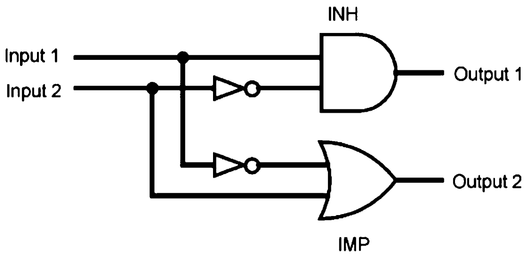

Figure 55. Combinational logic circuit with INH and IMP outputs.

Similarly, the output information was monitored in the form of change in absorbance at 554 nm (Output 1) and 325 nm (Output 2) by processing Inputs 1 and 2 as an addition of F^- and H^+, respectively. The Outputs 1 and 2 displayed a Boolean value of “1” only when F^- ions were present in the solution; in all other cases both output signals showed Boolean value “0”. Thus, both the output information signified an INH logic circuit.

Further, a more complex system was enumerated using a four-input system. This could be a first of its kind in which four-input systems have been used to obtain a molecular logic gate. The addition of Cu^{2+} ions, F^- ions, H_2O and H^+ provided the Inputs 1, 2, 3 and 4, respectively. The output was obtained by monitoring the change in fluorescence emission at 463 nm (Table 24). The combinatorial output information follows the logic circuit shown in Figure 56.

Table 24. Truth table for a combinatorial logic gate.

Input 1 (Cu^{2+})	Input 2 (F^-)	Input 3 (H_2O)	Input 4 (H^+)	Output (463 nm)
0	0	0	0	1
0	0	0	1	1
0	0	1	0	1
0	0	1	1	1
0	1	0	0	0
0	1	0	1	1
0	1	1	0	0
0	1	1	1	1
1	0	0	0	0
1	0	0	1	0
1	0	1	0	1
1	0	1	1	1
1	1	0	0	0
1	1	0	1	0
1	1	1	0	0
1	1	1	1	1

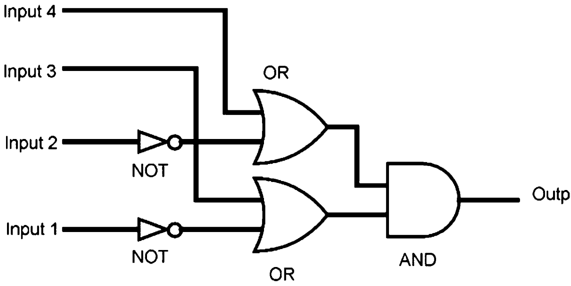

Figure 56. Combinatorial logic circuit with four input system.

More complex molecules reported by Kumar et al.[97,103] can detect Fe^{2+} ions; this type of sensor may be useful for the early detection of diseases such as anaemia, and these organic molecules could be used to monitor the iron content in the blood. In addition, the challenging task of monitoring the intracellular Ca^{2+} ion concentration could be effectively executed with the Ca^{2+}-ion detectable organic molecules.[98] A variety of organic sensors are available for the detection and quantification of Hg^{2+} ions;[99,101,104,105,109] these sytems can, in turn, be developed as devices for the selective detection of Hg^{2+} ions.

5. Applications of Molecular Logic Gates

The significance of new field always depends on how it is useful for real life applications and how well it is used in interdisciplinary fields. If the new field can create a positive impact on the people, then the efforts of scientific community to develop this field will be successful.

We know that sensor molecules can behave as rudimentary molecular logic gates, and as such it must possess a minimum of two different states with measurable distinct output properties. The first when it is free of input ions and the second state occurs when the sensor is engaged with the input ions. If the output signal increases with the increasing input ions, then it represents the Boolean value “1” (or the system is said to be “ON”). If the output signal decreases or does not changes with the increasing input ions then it is designated with the Boolean value “0” (also known as the system is “OFF’). Based on this approach various molecular-logic-based computational operations have been developed. Though this field is currently at the state proof-of-concept, it has enough mature application in various areas. Thus, the field of molecular computation has changed its perception from "impossible" to "it is possible, but with less capabilities".

The major advantage of these molecular computational systems as compared to semiconductor computational systems is their size. These molecular computational systems can be extended to the nanoscale, a size that semiconductor systems cannot reach as they are too large. For an instance, it is impossible to measure the concentration of Ca^{2+} ions using semiconductor-based devices within a cell or in the tissue, whereas it can be easily monitored by using Ca^{2+} chelating ligands with the help of YES logic gate. Therefore, it is significant to discuss the application of molecular logic gates that have been developed by the use of ion receptors/sensors; some of them are discussed in the following subsections.

5.1. Blood electrolyte measurement

Blood electrolytes such as Na^+, K^+, Ca^{2+} and H^+ can be measured with a commercial cellulose fibre mat (Figure 57). This fibre mat is made up of different fluorescent organic sensors (**44**–**47**) that can detect these ions. The ion-bound organic sensors show strong fluorescence enhancement, which can be directly converted to give level of these ions in the blood.[112–114]

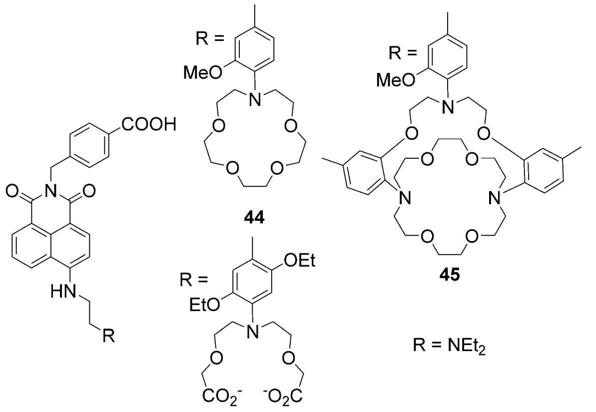

44 **45** **46** **47**

5.2. Nuclear waste monitors

Nuclear waste monitoring is very significant as it can cause hazardous mutations in the biological and ecological systems. Subsequently, there has been a significant amount of research on detection of radioactive isotopes such as ^{137}Cs. Calixarene derivatives, which display fluorescence enhancement upon binding with ^{137}Cs, have been utilised for the detection of this isotope.[115]

5.3. Marine toxin sensors

Molecular logic gates can be used for the detection of marine toxins, such as saxitoxin. A receptor with an azacrown ether containing Na^+ ions was able to bind the saxitoxin, resulting in a saxitoxin-driven YES logic gate.[116]

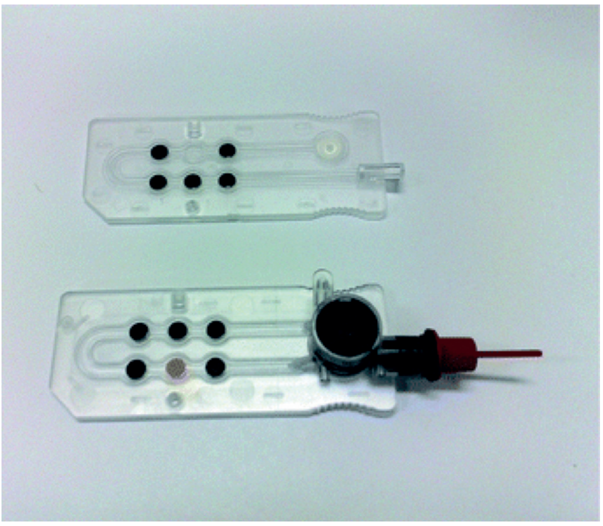

Figure 57. Commercial fibre mats sold by Optimedical Inc. for blood electrolyte measurements[11] (reproduced from reference [11] with permission from the RSC).

5.4. Ion tracking system within the cell

Semiconductor devices are too large to measure Ca^{2+} ions inside a cell. Therefore, Ca^{2+} sensors, such as **48**, can be used to detect the concentration of Ca^{2+} ions quantitatively within the cell. The Ca^{2+} ion induces enhancement in fluorescence excitation spectrum which represents a YES logic gate.[117,118] Similarly the sensing of H^+, Na^+, Mg^{2+} and Zn^{2+} by biocompatible computational devices has been achieved for the detection of these ions within cells.[119–123]

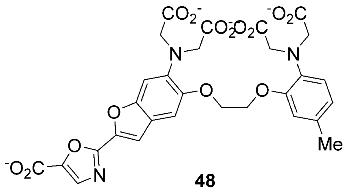

48

5.5. Biological electrodes to measure membrane potential

A cell possesses many significant properties, one of which is the membrane potential, can also be measured with molecular logic gates. Though electrophysiology is available to measure the membrane potential, the insertion of the electrode tip into the membrane is not easy. On the other hand, molecules such as **49** show large enhancement in the fluorescence when the

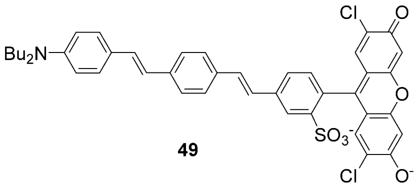

49

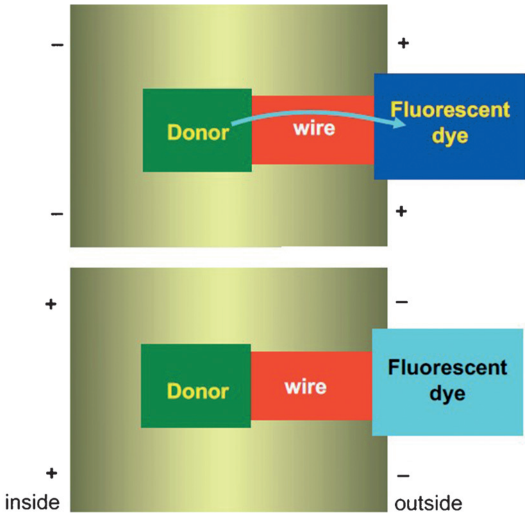

Figure 58. Fluorescent signalling by sensor **49** with the change in electrode potential.[126] (reproduced from reference [126] with permission from the Nature Publishing Group).

external potential of the membrane becomes negative (depolarisation of cell) as shown in Figure 58.[124,125]

5.6. Intracellular thermometers

The intracellular temperature can be measured by using organic molecules that can detect the rise in the temperature of mitochondria due to oxidative phosphorylation uncoupling. The organic molecule show enhanced fluorescence due to the change in temperature.[127]

Though only handful of application are present as of now, the field of molecular logic gates is gaining significance owing to their small size. In near future we can expect a larger number of interdisciplinary applications and robust ideas to replace the semiconductor devices.

6. Conclusion

Based on above discussions, it is clear that the molecular logic gates in which anions are utilised as one of the input signals have been developed extensively during recent years. As a result of an enumerable rise in the cost and physical limits involved in the continual conventional downsizing of microelectronics, researchers are now looking into other alternatives and molecular electronics, involving chemical components, could be a good opportunity that permits a bottom-up approach to synthesise nanoscale electronics. This review summarises the recent progress and key findings in the development of anion sensors as molecular logic gates. This new and promising field, based on engineering of organic molecules with desired logic gate performances, has many advantages, such as memory units/complex logic operations and the potential to be translated for future molecular-based computing applications. After de Silva et al.[5] postulated the possibility of molecular logic gates in 1993, researchers have explored two/three input systems by the addition of anion or cations as the inputs.

Since as most of the articles reported in the literature have discussed theoretical possibility of molecular logic circuits, it is a complex and challenging task to use them in day-to-day life. Though, molecular computation is rudimentary when compared to semiconductor computations, it already has promising useful applications. Molecular logic gates have been utilised for intracellular applications, such as intracellular imaging, monitoring the membrane potential and blood electrolyte monitoring. In addition, recent advances in marine toxin sensors and nuclear waste monitors have been developed with the help of molecular logic gates. However, for complex practical applications and molecular computing techniques significant research still needs to be carried out. Such complex applications might be achievable in the near future, but for the time being molecular computing is in its infancy and is not a substitute for the semiconductor-based computaters.

Therefore, more challenges are waiting ahead toward the implementation of molecular electronics into devices and if successful they may replace semiconductor computational devices. In addition to computational applications, molecular electronics might have other significance in areas such as intelligent environmental and biomedical sensing and smart drug delivery systems, which includes combined sensing and drug delivery functions.

Acknowledgements

The authors acknowledge the financial support from SERB-DST, India (YSS/2015/000013), DST, India (DST-TM-WTI-2K14-213), DST Nanomission, India (SR/NM/NS-20/2014), and Prof. Geetha Balakrishna, Director, CNMS, Jain University, Bangalore for providing research facility and infrastructure.

Keywords: anion receptors · chemical inputs · computer components · logic gates · molecular computation

[1] M. A. Reed, J. M. Tour, *Sci. Am.* **2000**, *282*, 86–93.
[2] J. M. Tour, *Acc. Chem. Res.* **2000**, *33*, 791–804.
[3] L. Sun, Y. A. Diaz-Fernandez, T. A. Gschneidtner, F. Westerlund, S. Lara-Avila, K. Moth-Poulsen, *Chem. Soc. Rev.* **2014**, *43*, 7378–7411.
[4] J. M. Tour, *Chem. Rev.* **1996**, *96*, 537–554.
[5] P. A. de Silva, N. H. Q. Gunaratne, C. P. McCoy, *Nature* **1993**, *364*, 42–44.
[6] A. P. de Silva, *Chem. Asian J.* **2011**, *6*, 750–766.
[7] A. P. de Silva, *J. Phys. Chem. Lett.* **2011**, *2*, 2865–2871.
[8] A. P. de Silva, C. M. Dobbin, T. P. Vance, B. Wannalerse, *Chem. Commun.* **2009**, 1386–1388.
[9] D. C. Magri, G. J. Brown, G. D. McClean, A. P. de Silva, *J. Am. Chem. Soc.* **2006**, *128*, 4950–4951.
[10] A. Prasanna de Silva, N. D. McClenaghan, *J. Am. Chem. Soc.* **2000**, *122*, 3965–3966.
[11] A. P. de Silva, T. P. Vance, M. E. S. West, G. D. Wright, *Org. Biomol. Chem.* **2008**, *6*, 2468–2481.
[12] P. L. Gentili, *J. Phys. Chem. A* **2008**, *112*, 11992–11997.
[13] H. Komatsu, S. Matsumoto, S. Tamaru, K. Kaneko, M. Ikeda, I. Hamachi, *J. Am. Chem. Soc.* **2009**, *131*, 5580–5585.
[14] M. Moshe, J. Elbaz, I. Willner, *Nano Lett.* **2009**, *9*, 1196–1200.
[15] J. Elbaz, M. Moshe, I. Willner, *Angew. Chem. Int. Ed.* **2009**, *48*, 3834–3837; *Angew. Chem.* **2009**, *121*, 3892–3895.
[16] F. Pu, C. Wang, D. Hu, Z. Huang, J. Ren, S. Wang, X. Qu, *Mol. Biosyst.* **2010**, *6*, 1928–1932.

[17] F. Pu, J. Ren, X. Yang, X. Qu, *Chem. Eur. J.* **2011**, *17*, 9590 – 9594.
[18] S. Angelos, Y. W. Yang, N. M. Khashab, J. F. Stoddart, J. I. Zink, *J. Am. Chem. Soc.* **2009**, *131*, 11344 – 11346.
[19] T. H. Lee, J. I. Gonzalez, J. Zheng, R. M. Dickson, *Acc. Chem. Res.* **2005**, *38*, 534 – 541.
[20] J. E. Green, J. W. Choi, A. Boukai, Y. Bunimovich, E. Johnston-Halperin, E. Delonno, Y. Luo, B. A. Sheriff, K. Xu, Y. S. Shin, H. R. Tseng, J. F. Stoddart, J. R. Heath, *Nature* **2007**, *445*, 414 – 417.
[21] T. Kudernac, N. Katsonis, W. R. Browne, B. L. Feringa, *J. Mater. Chem.* **2009**, *19*, 7168 – 7177.
[22] A. P. de Silva, N. D. McClenaghan, *Chem. Eur. J.* **2004**, *10*, 574 – 586.
[23] A. P. de Silva, S. Uchiyama, *Nat. Nanotechnol.* **2007**, *2*, 399 – 410.
[24] T. Kumeria, J. Yu, M. Alsawat, M. D. Kurkuri, A. Santos, A. D. Abell, D. Losic, *Adv. Mater.* **2015**, *27*, 3019 – 3024.
[25] F. Meng, Y. M. Hervault, Q. Shao, B. Hu, L. Norel, S. Rigaut, X. Chen, *Nat. Commun.* **2014**, *5*, 3023.
[26] J. M. Tour, W. L. Van Zandt, C. P. Husband, S. M. Husband, L. S. Wilson, P. D. Franzon, D. P. Nackashi, *IEEE Trans. Nanotechnol.* **2002**, *1*, 100 – 109.
[27] P. A. Gale, *Coord. Chem. Rev.* **2000**, *199*, 181 – 233.
[28] T. Gunnlaugsson, H. D. Ali, M. Glynn, P. E. Kruger, G. M. Hussey, F. M. Pfeffer, C. M. dos Santos, J. Tierney, *J. Fluoresc.* **2005**, *15*, 287 – 299.
[29] A. Kumar, M. Chhatwal, R. D. Gupta, S. K. Awasthi, *RSC Adv.* **2015**, *5*, 5217 – 5220.
[30] R. Custelcean, *Chem. Soc. Rev.* **2010**, *39*, 3675 – 3685.
[31] T. H. Rehm, C. Schmuck, *Chem. Soc. Rev.* **2010**, *39*, 3597 – 3611.
[32] H. Juwarker, K. S. Jeong, *Chem. Soc. Rev.* **2010**, *39*, 3664 – 3674.
[33] J. T. Davis, O. Okunola, R. Quesada, *Chem. Soc. Rev.* **2010**, *39*, 3843 – 3862.
[34] A. P. Davis, J.-B. Joos, *Coord. Chem. Rev.* **2003**, *240*, 143 – 156.
[35] J. M. Llinares, D. Powell, K. Bowman-James, *Coord. Chem. Rev.* **2003**, *240*, 57 – 75.
[36] R. Martínez-Máñez, F. Sancenon, *J. Fluoresc.* **2005**, *15*, 267 – 285.
[37] T. Gunnlaugsson, M. Glynn, G. M. Tocci, P. E. Kruger, F. M. Pfeffer, *Coord. Chem. Rev.* **2006**, *250*, 3094 – 3117.
[38] S. Kubik, *Chem. Soc. Rev.* **2009**, *38*, 585 – 605.
[39] Q. Zhao, F. Li, C. Huang, *Chem. Soc. Rev.* **2010**, *39*, 3007 – 3030.
[40] A. F. Li, J. H. Wang, F. Wang, Y. B. Jiang, *Chem. Soc. Rev.* **2010**, *39*, 3729 – 3745.
[41] E. Galbraith, T. D. James, *Chem. Soc. Rev.* **2010**, *39*, 3831 – 3842.
[42] S. Kubik, *Chem. Soc. Rev.* **2010**, *39*, 3648 – 3663.
[43] Z. Xu, S. K. Kim, J. Yoon, *Chem. Soc. Rev.* **2010**, *39*, 1457 – 1466.
[44] M. E. Moragues, R. Martinez-Manez, F. Sancenon, *Chem. Soc. Rev.* **2011**, *40*, 2593 – 2643.
[45] P. Dydio, D. Lichosyt, J. Jurczak, *Chem. Soc. Rev.* **2011**, *40*, 2971 – 2985.
[46] Y. Zhou, J. F. Zhang, J. Yoon, *Chem. Rev.* **2014**, *114*, 5511 – 5571.
[47] M. D. Best, S. L. Tobey, E. V. Anslyn, *Coord. Chem. Rev.* **2003**, *240*, 3 – 15.
[48] V. Amendola, L. Fabbrizzi, E. Monzani, *Chem. Eur. J.* **2004**, *10*, 76 – 82.
[49] Q.-Y. Cao, Z.-C. Wang, M. Li, J.-H. Liu, *Tetrahedron Lett.* **2013**, *54*, 3933 – 3936.
[50] K. Ghosh, I. Saha, *J. Mol. Struct.* **2013**, *1042*, 57 – 65.
[51] D. Zhang, X. Jiang, Z. Dong, H. Yang, A. Martinez, G. Gao, *Tetrahedron* **2013**, *69*, 10457 – 10462.
[52] P. Das, M. K. Kesharwani, A. K. Mandal, E. Suresh, B. Ganguly, A. Das, *Org. Biomol. Chem.* **2012**, *10*, 2263 – 2271.
[53] P. Das, A. K. Mandal, M. K. Kesharwani, E. Suresh, B. Ganguly, A. Das, *Chem. Commun.* **2011**, *47*, 7398 – 7400.
[54] Madhuprasad, D. R. Trivedi, *ChemPlusChem* **2014**, *79*, 1001 – 1008.
[55] P. Sokkalingam, C. H. Lee, *J. Org. Chem.* **2011**, *76*, 3820 – 3828.
[56] Y. Bao, B. Liu, H. Wang, J. Tian, R. Bai, *Chem. Commun.* **2011**, *47*, 3957 – 3959.
[57] S. Sumiya, T. Doi, Y. Shiraishi, T. Hirai, *Tetrahedron* **2012**, *68*, 690 – 696.
[58] H.-T. Niu, X. Jiang, J. He, J.-P. Cheng, *Tetrahedron Lett.* **2009**, *50*, 6668 – 6671.
[59] S. Sharma, M. S. Hundal, G. Hundal, *Org. Biomol. Chem.* **2013**, *11*, 654 – 661.
[60] M.-J. Peng, Y. Guo, X.-F. Yang, L.-Y. Wang, J. An, *Dyes Pigm.* **2013**, *98*, 327 – 332.
[61] M. R. Ajayakumar, K. Mandal, K. Rawat, D. Asthana, R. Pandey, A. Sharma, S. Yadav, S. Ghosh, P. Mukhopadhyay, *ACS Appl. Mater. Interfaces* **2013**, *5*, 6996 – 7000.
[62] X. Zheng, W. Zhu, D. Liu, H. Ai, Y. Huang, Z. Lu, *ACS Appl. Mater. Interfaces* **2014**, *6*, 7996 – 8000.
[63] Madhuprasad, N. Swathi, J. R. Manjunatha, U. K. Das, A. N. Shetty, D. R. Trivedi, *New J. Chem.* **2014**, *38*, 1484 – 1492.
[64] Z. H. Lin, Y. G. Zhao, C. Y. Duan, B. G. Zhang, Z. P. Bai, *Dalton Trans.* **2006**, 3678 – 3684.
[65] Z. H. Lin, S. J. Ou, C. Y. Duan, B. G. Zhang, Z. P. Bai, *Chem. Commun.* **2006**, 624 – 626.
[66] V. Bhalla, Roopa, M. Kumar, *Org. Lett.* **2012**, *14*, 2802 – 2805.
[67] Q. Li, Z. Wang, J. Xu, Y. Yue, S. Shao, *RSC Adv.* **2014**, *4*, 34470.
[68] J. Andréasson, U. Pischel, *Chem. Soc. Rev.* **2010**, *39*, 174 – 188.
[69] Q. Lin, Q.-P. Yang, B. Sun, J.-C. Lou, T.-B. Wei, Y.-M. Zhang, *RSC Adv.* **2015**, *5*, 11786 – 11790.
[70] W. C. Lin, S. K. Fang, J. W. Hu, H. Y. Tsai, K. Y. Chen, *Anal. Chem.* **2014**, *86*, 4648 – 4652.
[71] S. Madhu, S. K. Basu, S. Jadhav, M. Ravikanth, *Analyst* **2013**, *138*, 299 – 306.
[72] S. Madhu, M. Ravikanth, *Inorg. Chem.* **2014**, *53*, 1646 – 1653.
[73] H. N. Lee, N. J. Singh, S. K. Kim, J. Y. Kwon, Y. Y. Kim, K. S. Kim, J. Yoon, *Tetrahedron Lett.* **2007**, *48*, 169 – 172.
[74] W. Lu, M. Zhang, K. Liu, B. Fan, Z. Xia, L. Jiang, *Sens. Actuators B* **2011**, *160*, 1005 – 1010.
[75] Y. Qu, S. Qu, L. Yang, J. Hua, D. Qu, *Sens. Actuators B* **2012**, *173*, 225 – 233.
[76] M. R. Ajayakumar, G. Hundal, P. Mukhopadhyay, *Chem. Commun.* **2013**, *49*, 7684 – 7686.
[77] L. Wang, B. Li, L. Zhang, P. Li, H. Jiang, *Dyes Pigm.* **2013**, *97*, 26 – 31.
[78] H. Tavallali, G. Deilamy-Rad, A. Parhami, N. Hasanli, *J. Hazard. Mater.* **2014**, *266*, 189 – 197.
[79] W. Lu, D. Chen, H. Jiang, L. Jiang, Z. Shen, *J. Polym. Sci. Part A* **2012**, *50*, 590 – 598.
[80] J. Liu, X. He, J. Zhang, T. He, L. Huang, J. Shen, D. Li, H. Qiu, S. Yin, *Sens. Actuators B* **2015**, *208*, 538 – 545.
[81] V. Luxami, S. Kumar, *New J. Chem.*, **2008**, *32,* 2074 – 2079.
[82] K. K. Upadhyay, A. Kumar, R. K. Mishra, T. M. Fyles, S. Upadhyay, K. Thapliyal, *New J. Chem.* **2010**, *34*, 1862 – 1866.
[83] J. Wang, C.-S. Ha, *Sens. Actuators B* **2010**, *146*, 373 – 380.
[84] M. Shahid, P. Srivastava, A. Misra, *New J. Chem.* **2011**, *35*, 1690.
[85] V. Luxami, S. Kumar, *Dalton Trans.* **2012**, *41*, 4588 – 4593.
[86] P. Xue, R. Lu, J. Jia, M. Takafuji, H. Ihara, *Chem. Eur. J.* **2012**, *18*, 3549 – 3558.
[87] V. Uahengo, B. Xiong, N. Zhou, P. Cai, K. Hu, G. Cheng, *Chin. J. Chem.* **2012**, *30*, 1702 – 1708.
[88] X. Wang, H. Yang, *Appl. Surf. Sci.* **2013**, *277*, 257 – 262.
[89] M. A. Kaloo, J. Sankar, *New J. Chem.* **2014**, *38*, 923 – 926.
[90] S. Areti, J. K. Khedkar, R. Chilukula, C. P. Rao, *Tetrahedron Lett.* **2013**, *54*, 5629 – 5634.
[91] Q. Lin, X. Liu, T.-B. Wei, Y.-M. Zhang, *Sens. Actuators B* **2014**, *190*, 459 – 463.
[92] V. García, A. Fernández-Lodeiro, R. Lamelas, A. Macías, R. Bastida, E. Bértolo, C. Núñez, *Dyes Pigm.* **2014**, *110*, 143 – 151.
[93] S. Pramanik, V. Bhalla, M. Kumar, *ACS Appl. Mater. Interfaces* **2014**, *6*, 5930 – 5939.
[94] B. Kumar, M. A. Kaloo, A. Raja Sekhar, J. Sankar, *Dalton Trans.* **2014**, *43*, 16164 – 16168.
[95] V. Luxami, A. S. Gupta, K. Paul, *New J. Chem.* **2014**, *38*, 2841 – 2846.
[96] M. Kluciar, R. Ferreira, B. de Castro, U. Pischel, *J. Org. Chem.* **2008**, *73*, 6079 – 6085.
[97] M. Kumar, R. Kumar, V. Bhalla, *Tetrahedron Lett.* **2010**, *51*, 5559 – 5562.
[98] K.-C. Chang, I.-H. Su, Y.-Y. Wang, W.-S. Chung, *Eur. J. Org. Chem.* **2010**, 4700 – 4704.
[99] A. Kumar, V. Kumar, K. K. Upadhyay, *Tetrahedron Lett.* **2011**, *52*, 6809 – 6813.
[100] K. Kaur, V. K. Bhardwaj, N. Kaur, N. Singh, *Inorg. Chem. Commun.* **2012**, *26*, 31 – 36.
[101] Z. Dong, X. Tian, Y. Chen, J. Hou, Y. Guo, J. Sun, J. Ma, *Dyes Pigm.* **2013**, *97*, 324 – 329.
[102] S. Goswami, A. Manna, S. Paul, K. Aich, A. K. Das, S. Chakraborty, *Dalton Trans.* **2013**, *42*, 8078 – 8085.
[103] R. Kumar, V. Bhalla, M. Kumar, *Dalton Trans.* **2013**, *42*, 8808 – 8814.
[104] Z. Dong, X. Tian, Y. Chen, J. Hou, J. Ma, *RSC Adv.* **2013**, *3*, 2227 – 2233.

[105] T. Mistri, R. Alam, M. Dolai, S. Kumar Mandal, P. Guha, A. Rahman Khuda-Bukhsh, M. Ali, *Eur. J. Inorg. Chem.* **2013**, 5854 – 5861.
[106] L. Wang, B. Li, L. Zhang, Y. Luo, *Dalton Trans.* **2013**, *42*, 459 – 465.
[107] A. Gogoi, S. Samanta, G. Das, *Sens. Actuators B* **2014**, *202*, 788 – 794.
[108] A. K. Mahapatra, S. K. Manna, C. D. Mukhopadhyay, D. Mandal, *Sens. Actuators B* **2014**, *200*, 123 – 131.
[109] S. Madhu, R. Kalaiyarasi, S. K. Basu, S. Jadhav, M. Ravikanth, *J. Mater. Chem. C* **2014**, *2*, 2534 – 2544.
[110] A. K. Mahapatra, S. K. Manna, K. Maiti, R. Maji, C. D. Mukhopadhyay, D. Sarkar, T. K. Mondal, *RSC Adv.* **2014**, *4*, 36615 – 36622.
[111] Y. Fu, Q. C. Feng, X. J. Jiang, H. Xu, M. Li, S. Q. Zang, *Dalton Trans.* **2014**, *43*, 5815 – 5822.
[112] A. P. de Silva, H. Q. N. Gunaratne, J.-L. Habib-Jiwan, C. P. McCoy, T. E. Rice, J.-P. Soumillion, *Angew. Chem. Int. Ed. Engl.* **1995**, *34*, 1728 – 1731; *Angew. Chem.* **1995**, *107*, 1889 – 1891.
[113] H. He, M. A. Mortellaro, M. J. P. Leiner, R. J. Fraatz, J. K. Tusa, *J. Am. Oil Chem. Soc.* **2003**, *125*, 1468 – 1469.
[114] J. K. Tusa, H. He, *J. Mater. Chem.* **2005**, *15*, 2640.
[115] H.-F. Ji, G. M. Brown, R. Dabestani, *Chem. Commun.* **1999**, 609 – 610.
[116] P. Kele, J. Orbulescu, R. E. Gawley, R. M. Leblanc, *Chem. Commun.* **2006**, 1494 – 1496.
[117] G. Grynkiewicz, M. Poenie, R. Y. Tsien, *J. Biol. Chem.* **1985**, *260*, 3440 – 3450.
[118] R. Y. Tsien, *Am. J. Physiol. Cell Physiol.* **1992**, *263*, C723 – C728.
[119] N. Klonis, W. Sawyer, *J. Fluoresc.* **1996**, *6*, 147 – 157.
[120] A. Minta, R. Y. Tsien, *J. Biol. Chem.* **1989**, *264*, 19449 – 19457.
[121] B. Raju, E. Murphy, L. A. Levy, R. D. Hall, R. E. London, *Am. J. Physiol. Cell Physiol.* **1989**, *256*, C540 – 548.
[122] E. Tamanini, A. Katewa, L. M. Sedger, M. H. Todd, M. Watkinson, *Inorg. Chem.* **2009**, *48*, 319 – 324.
[123] A. T. Harootunian, J. P. Kao, B. K. Eckert, R. Y. Tsien, *J. Biol. Chem.* **1989**, *264*, 19458 – 19467.
[124] E. W. Miller, J. Y. Lin, E. P. Frady, P. A. Steinbach, W. B. Kristan, R. Y. Tsien, *Proc. Natl. Acad. Sci. USA* **2012**, *109*, 2114 – 2119.
[125] J. E. González, R. Y. Tsien, *Chem. Biol.* **1997**, *4*, 269 – 277.
[126] A. P. de Silva, *Nat. Chem.* **2012**, *4*, 440 – 441.
[127] C. Gota, K. Okabe, T. Funatsu, Y. Harada, S. Uchiyama, *J. Am. Chem. Soc.* **2009**, *131*, 2766 – 2767.

Received: November 2, 2015